RIGA TECHNICAL UNIVERSITY

Jaroslavs Zarembo

RESEARCH AND DEVELOPMENT OF THE SYNCHRONOUS RELUCTANCE MOTOR TRACTION DRIVE

Summary of the Doctoral Thesis

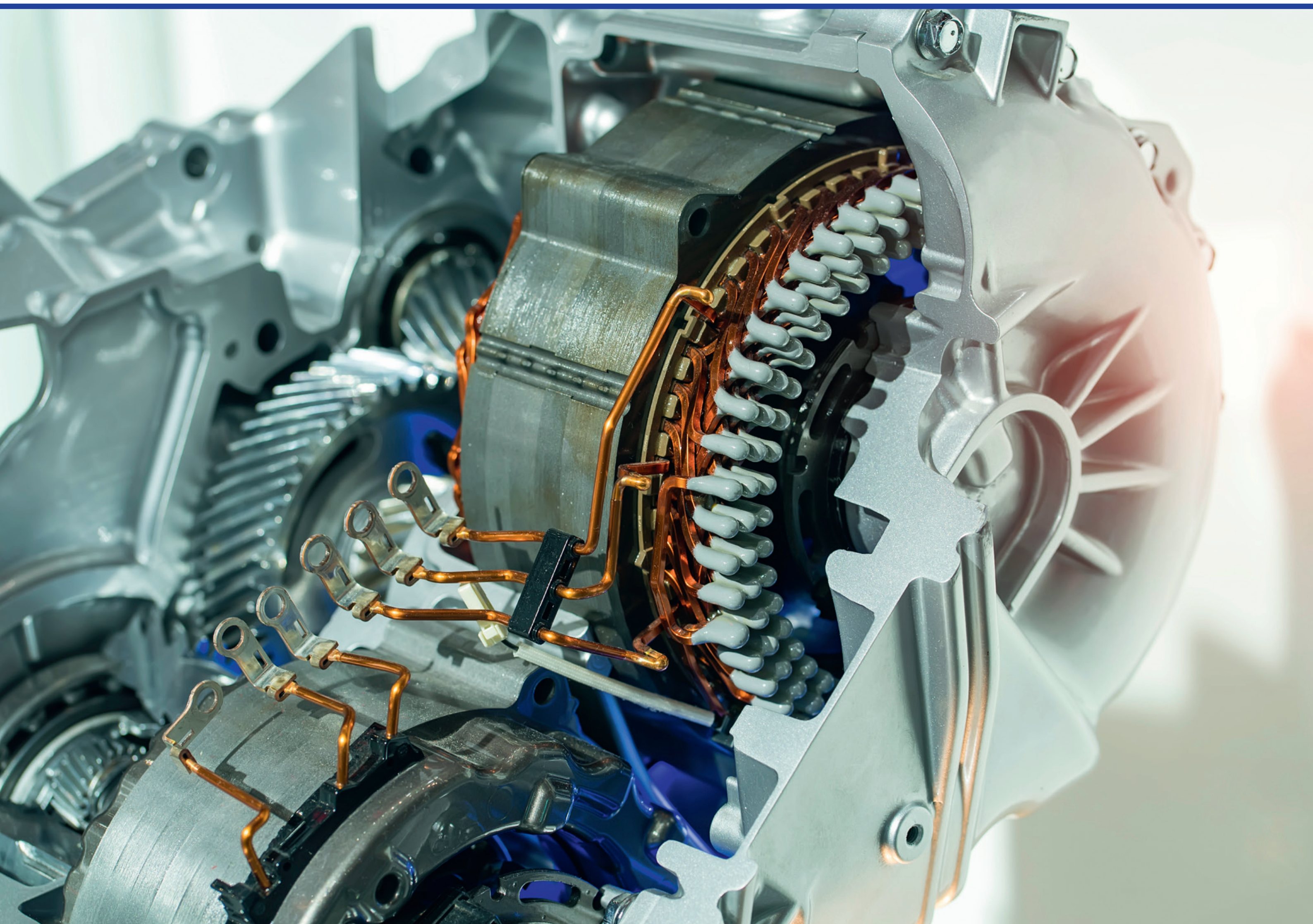

RTU Press
Riga 2022

RIGA TECHNICAL UNIVERSITY

Faculty of Electrical and Environmental Engineering

Institute of Industrial Electronics and Electrical Engineering

Jaroslavs Zarembo

Doctoral Student of Study Program “Computerized Control of Electrical Technologies”

RESEARCH AND DEVELOPMENT OF THE SYNCHRONOUS RELUCTANCE MOTOR TRACTION DRIVE

Summary of the Doctoral Thesis

Scientific Supervisor

Professor Dr. habil. sc. ing.

LEONĪDS RIBICKIS

RTU Press

Rīga 2022

Zarembo, J. Research and Development of the Synchronous Reluctance Motor Traction Drive. Summary of the Doctoral Thesis. – Riga: RTU Press, 2022. – 44 p.

Published in accordance with the decision of the Promotion "RTU P-14" of 21 April 2022, Minutes No. 210.11.

https://doi.org/10.7250/9789934227844
ISBN 978-9934-22-784-4 (pdf)

DOCTORAL THESIS PROPOSED TO RIGA TECHNICAL UNIVERSITY FOR THE PROMOTION TO THE SCIENTIFIC DEGREE OF DOCTOR OF SCIENCE

To be granted the scientific degree of Doctor of Science (Ph. D.), the present Doctoral Thesis has been submitted for the defence at the open meeting of RTU Promotion Council on June 16, 2022 at the Faculty of Electrical and Environmental Engineering of Riga Technical University, Azenes Street 12 k-1, Room 212.

OFFICIAL REVIEWERS

Professor Dr. habil. sc. ing. Janis Dirba
Riga Technical University

Dr. sc. ing. Svetlana Orlova
Institute of Physical Energetics, Latvia

Ph.D. Alecksey Anuchin
Moscow Power Engineering Institute, Russia

DECLARATION OF ACADEMIC INTEGRITY

I hereby declare that the Doctoral Thesis submitted for the review to Riga Technical University for the promotion to the scientific degree of Doctor of Science (Pf. D) is my own. I confirm that this Doctoral Thesis had not been submitted to any other university for the promotion to a scientific degree.

Name Surname ……………………………. (signature)

Date: ………………………

The Doctoral Thesis has been written in English. It consists of Introduction, 5 chapters, Conclusions, 58 figures, 12 tables, and 2 appendices; the total number of pages is 80, including appendices. The Bibliography contains 40 titles.

Contents

Introduction

Topic relevance

The problem of ecology and greenhouse emissions has become critical in the modern world. In cities, transport is the largest source of CO_2 and other emissions. The solution to the problem should be the transfer of the transport system of a large city to an electric drive. Electric transport reduces noise level, eliminates exhaust pollution, and helps to overcome dependence on oil by allowing electricity to be used for power, which, in turn, can be obtained from alternative sources. Addressing the issue, a special-purpose EU programme on reducing greenhouse gas emissions in urban transport by 60 % by 2050 has been adopted [1].

One of the existing transport types that can be used to achieve the set goal is a trolleybus. The trolleybus was first introduced in 1882, when Dr. Ernst Werner ran his bus in Berlin suburbs. Already in 1901, the world’s first passenger-carrying trolleybus operated in Bielathal, in Germany. However, later with abundant amount of oil and lack of environmental regulations urban electric transport became less economically viable and eventually in many cities stopped being used. Fossil fuel was cheap, and overhead traction grid wires were thought to spoil the view and require expensive maintenance [2]. Nowadays trolleybus infrastructure remains in approximately 300 cities in the world, but due to environmental policy has changed over the past decades and trolleybuses can again find their place in the infrastructure of the new green community.

Many studies have been carried out to find new solutions to improve the performance of a trolleybus. The main trends were focusing on ensuring the ability to drive autonomously on some route sections and saving energy by installing on-board energy storage devices. Storage systems based on supercapacitors or batteries have proven their efficiency, however, their installation leads to a significant rise in the cost of a set of electrical equipment [3]. An alternative could be a complete replacement of trolleybuses with electric buses, but this entails a complete restructuring of the city's infrastructure to ensure fast charging. Another solution could be a hybrid trolleybus system with in motion charging on a limited section of the track [4]. Thus, the general trend in the development of the trolleybus is the installation of on-board energy storage devices.

With the emergence of vehicles with on-board energy sources, the issue of power reserve comes to the forefront. Portable energy storage devices with high capacity, such as lithium-ion batteries, fuel cells, and supercapacitors, are the most expensive part of an electric drive, therefore, the most important task of a traction system is high efficiency rate. Regardless of the used energy source, total consumed energy for the movement of the vehicle directly depends on the efficiency of the motor in a whole working range.

In most of modern trolleybus traction systems conventional induction motors (IM) are used. The advantages of the IM drive are reliability, relatively low cost of the set, and the robust and proven control system. Though, nowadays high efficiency demands are hardly met by this type of drive system. Another solution is permanent magnet synchronous motor (PMSM) drive that provides the best indicators of power-to-mass ratio, as well as the best possible efficiency [5]. Drawbacks of PMSM are high cost of permanent magnets, as well as the dependence on a monopoly supplier. Both mentioned options are already well known and widely used in traction. However, introduction of alternative traction motor drive topologies could lead to optimisation of working parameters for a specific use case.

Potentially promising solution is the use of synchronous electric motors without active elements in the rotor. This approach reduces material costs, increases efficiency due to the absence of resistive losses in the rotor, and simplifies the manufacturing process. The most commonly topologies are switched reluctance motor (SRM) and synchronous reluctance motor (SynRM).

SRM is gaining popularity nowadays but has several disadvantages such as relatively low torque density, higher torque ripple, and acoustic noise [6]. Acoustic noise and torque ripple are restraining factors in the development of this type of electric motors. SynRM is less prone to the inherent disadvantages of SRM. In addition, the electric motor uses a distributed winding, which is classical for IM, which makes it possible to retain the topology of the power inverter [7]. However, due to nonlinearity of the characteristics, the design process of SynRM and the development of control system for such machines are more complex tasks.

In traction applications, SynRM is a good alternative for induction motors. While it was introduced in 1923, only nowadays due to improvements in computational power of microprocessors and more sophisticated computer aided analysis methods it is becoming more widespread [8].

The aim and tasks of the Thesis

The main aim of the Doctoral Thesis is the design, development, and testing of an electric drive based on SynRM and a two-level frequency inverter for traction application.

The tasks are:

- design of the electric motor;
- production of electric motor prototype;

- creation of a control system in a Matlab Simulink environment;
- development and deployment of embedded software for the microcontroller;
- testing of the produced electric motor with deployed control system on a laboratory setup.

Novelty of the Doctoral Thesis

Development of robust and precise control algorithm of the SynRM traction drive.

Innovative solutions developed in the Doctoral Thesis:

- A SynRM rotor geometry calculation algorithm considering the cross-saturation effect.
- Mathematical model of the trolleybus SynRM traction drive and its control algorithm, evaluated in laboratory conditions.
- Motor drive control software considering the cross-saturation effect, which allows for accurate motor control.

Practical value of the Doctoral Thesis

The development of an experimental electric SynRM drive was carried out by JSC "RER" within the framework of the EU project. The aim of the project was to develop, manufacture, and research an electric motor in the overall dimensions of an existing serial IM for a trolleybus. At the time of the start of the project, JSC "RER" produced only traction asynchronous electric motors. The result of the project was the development and testing of a new model of traction SynRM with the control system for trolleybus drive. The implementation of the project made it possible to gain experience in the production technology of a new type of electric motors.

The developed mathematical models and control software may be used in the development process of new drive systems.

Research software and hardware resources

The research work was performed using *Comsol* software to create the optimal SynRM rotor geometry, *Matlab Simulink* software to create the trolleybus SynRM propulsion and its control mathematical models, *LabVIEW* software to create a graphical control panel for laboratory testing, and *CCSTUDIO IDE* software (with TI Digital Motor Control Library) to develop embedded software for the microcontroller.

Publications

1. I. Dvornikovs, M. Marinbahs, J. Zarembo, E. Groza, and K. Ketners, "Investigation of traction motor dynamic using computer simulation and method of mutual loading of two pair motors," in *2019 16th Conference on Electrical Machines, Drives and Power Systems (ELMA)*, Varna, Bulgaria, 2019.
2. K. Gulbis, U. Brakanskis, E. Kamoliņš, and J. Zarembo, "Parameter Calculation Method of Synchronous Reluctance Motor Including Cross Magnetic Saturation," in *2020 IEEE 61th International Scientific Conference on Power and Electrical Engineering of Riga Technical University (RTUCON)*, Riga, Latvia, 2020.
3. V. Burenin, J. Zarembo, A. Žiravecka, and L. Ribickis, "Model of Laboratory Test Bench Setup for Testing Electrical Machines," in *2020 IEEE 61th International Scientific Conference on Power and Electrical Engineering of Riga Technical University (RTUCON)*, Riga, Latvia, 2020.
4. G. Kobenkins, M. Marinbahs, V. Burenin, J. Zarembo, A. Bizans, O. Sliskis, "Determination of the Level of Own Vibration of Geared Motor Boxes in Industrial Conditions," in *2021 IEEE 62st International Scientific Conference on Power and Electrical Engineering of Riga Technical University* , Riga, 2021.
5. V. Burenin, J. Zarembo, O. Krievs, and L. Ribickis, "Comparison of Synchronous Reluctance Motor and Induction Motor Efficiency Maps for Traction Application," in *RTUCON 2021*, Riga, Latvia, 2021.
6. G. Kobenkins, M. Marinbahs O. Sliskis, V. Burenin, J. Zarembo, "Carry Out of Strength Tests of Geared Motor Box as Part of a Frequency-Controlled Traction Electric Drive," in *17th Conference on Electrical Machines, Drives and Power Systems (ELMA 2021)*, Sofia, Bulgaria, 2021.
7. A. Potapovs, U. Brakanskis, M. Gorobecs, K. Gulbis, E. Kamoliņš, K. Sejejs, V. Burenin, J. Zarembo, "180 kW Synchronous Reluctance Motor for Mass Transit Electrical Traction Application," in *23rd European Conference on Power Electronics and Applications (EPE'21 ECCE Europe)*, Brussels, Belgium, 2021.
8. K. Gulbis, U. Brakanskis, E. Kamolins, M. Gorobecs, A. Potapovs, K. Sejejs, J. Zarembo and V. Burenin, "Analysis of Test Results of Developed Synchronous Reluctance Motor for Public Transport Application," *Latvian Journal of Physics and Technical Sciences,* 2021.

1. Analysis of Trolleybus Traction Requirements

Design process of the electric drive requires understanding dynamics of the vehicle under consideration, for it to properly set criteria for the traction at different speeds. This chapter describes underlying requirements for the dynamics of the trolleybus and construction of the traction characteristic.

1.1. Trolleybus Dynamics Requirements

In the case of this research, the vehicle under consideration is trolleybus. The trolleybus technical specification is provided by the manufacturer and is shown in Table 1.1. Trolleybus is 12 m single section.

Table 1.1

Trolleybus Parameters

Parameter	**Unit**	**Value**
Laden mass	[ton]	18.9
Gearbox number		9.84
Gearbox efficiency	%	97
Wheel diameter	[m]	0.88 (275/70R22.5)
Maximum working speed, at least	[km/h]	60
Acceleration till 45 km/h, at most	[s]	18
Maximum acceleration, at most	[m/s^2]	1.2
Maximum deceleration, at most	[m/s^2]	0.8
Rated voltage of overhead lines	[VDC]	550
Minimal voltage of overhead lines	[VDC]	400
Maximum voltage of overhead lines	[VDC]	700

In addition to the requirements in Table 1.1, trolleybus should abide by the following additional requirements to the dynamics:

- Electric drive should be able to sustain constant rated torque up to rated frequency of 50 Hz.
- Trolleybus should be able to sustain and reach the speed of 45 km/h at 12 ‰ of road inclination.
- At maximum speed of 60 km/h electric drive should have residual force of at least 10 % above resistive force.

Based on all mentioned requirements to the dynamics of the vehicle, traction characteristic is constructed, to be used for the design process and laboratory validation of the electric drive with SynRM.

1.2. Construction of Reference Traction Characteristic

In general, traction characteristic consists of three regions: constant torque, constant power ($T_{elm} \cdot \omega_m \cong const.$), and $T_{elm} \cdot \omega_m^2 \cong const.$, separation of regions is shown in Fig. 1.1 [9]. From this knowledge, traction characteristic for the trolleybus is constructed based on dynamics requirements and two transition points, one is 50 Hz, and the other is chosen so that at maximum speed residual torque requirement is fulfilled.

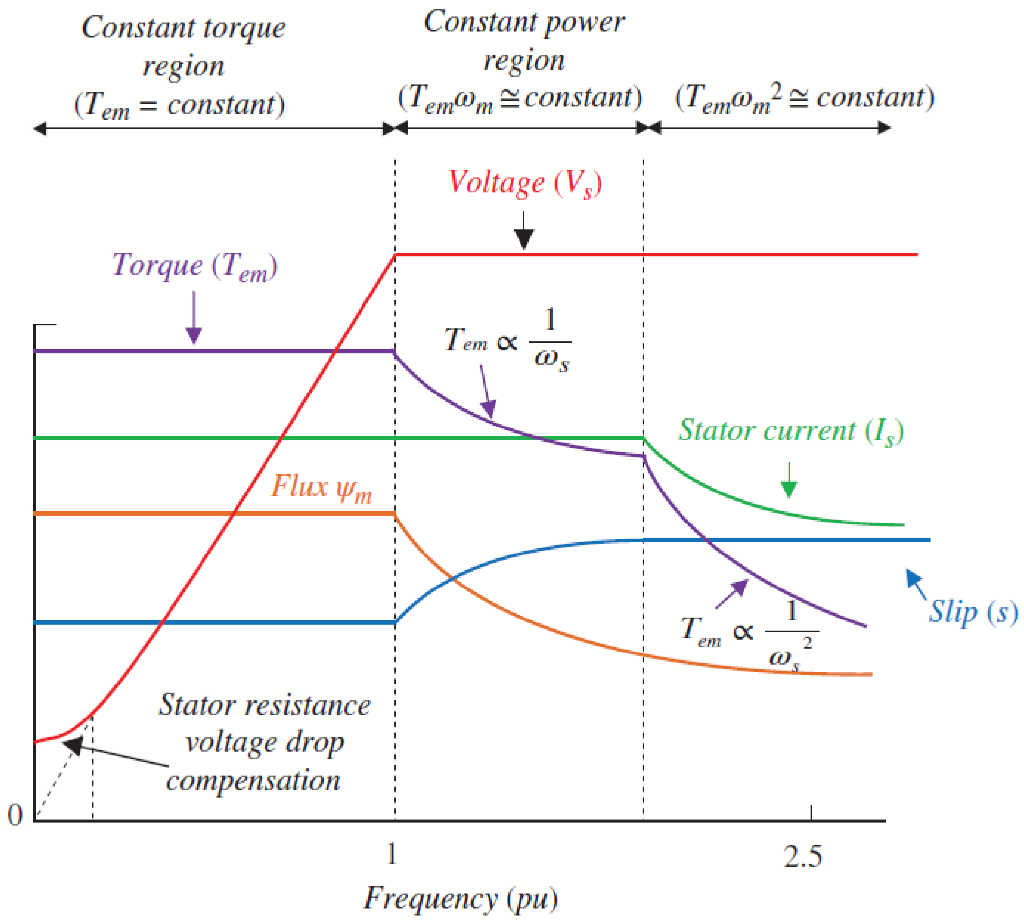

Fig. 1.1. Operating regions of the motor.

As the requirement for the acceleration is not very strict, there are several appropriate solutions for the provided dynamics requirements. Two optimal solutions are presented in Table 1.2. The first one provides a more agile movement for the trolleybus at the cost of higher output power, the second proposed solution has lower acceleration of the vehicle and a possibility to reduce the size of the motor.

Table 1.2

Proposed Solutions for Traction Characteristic

	Solution 1	Solution 2
P_{cnst} [kW]	180	170
	Horizontal road	
Time to 45 km/h, s	16.24	17.42
a_{max} [m/s^2]	1.02	0.96
Residual force at 60 km/h	26.3 %	19.3 %
Top speed, km/h	64.6	63.4
	12 ‰ Inclination	
Time to 45 km/h, s	19.27	20.99
a_{max} [m/s^2]	0.92	0.86
Residual force at 54 km/h	23.2 %	13.6 %
Top speed, km/h	56.9	55.7

Both solutions fulfil the requirements for movement. Solution 1 has higher reserve for operation, even being able to accelerate to 45 km/h in just under 18 seconds at inclined road, while Solution 2 has much less of a reserve.

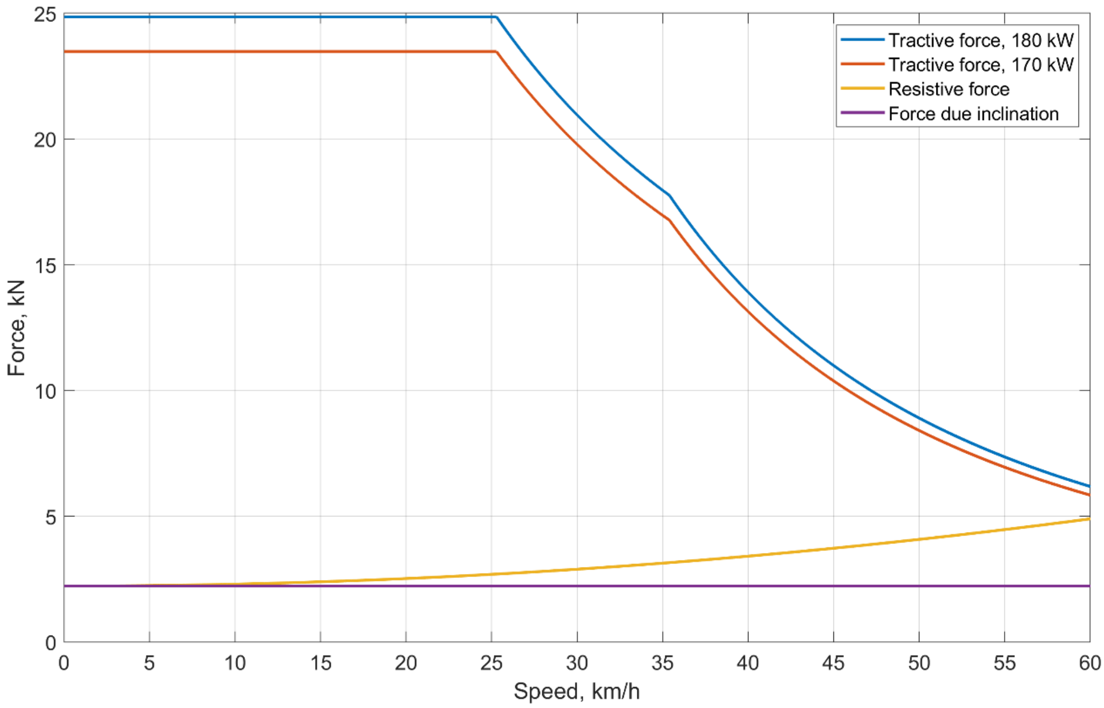

Fig. 1.2. Graphical representation of proposed traction characteristics.

Figure 1.2 is a graphical representation of proposed traction characteristics with resistive force and gravitational forces due to inclination.

2. Design of the SynRM Traction Drive

Design and production of the SynRM prototype is done as a part within the frame of the European Project. The design process has been published in The Latvian Journal of Physics and Technical Sciences [10]. Full description of the design and testing process was presented at the 23rd European Conference on Power Electronics and Applications [11]. This chapter gives a brief description of the design process with input data and results.

2.1. Working Principle of SynRM

The operation of a SynRM is based on the difference between the inductances of the direct and quadrature axes. This idea can be explained using Fig. 2.1 [12]. In this figure object "a" with anisotropic magnetic material has different (geometric) reluctances in the d-axis and q-axis. Whereas the isotropic magnetic material geometry in object "b" has similar in all directions.

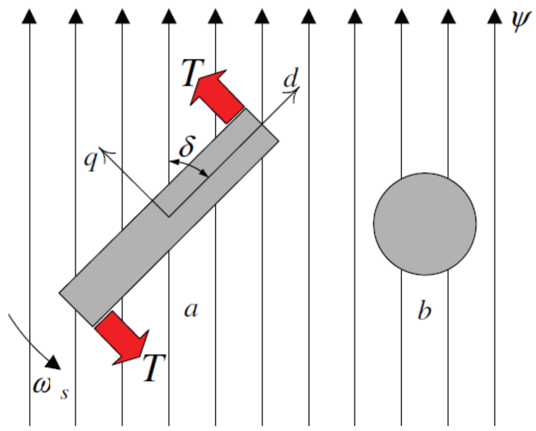

Fig. 2.1. An object with anisotropic (a) and isotropic (b) geometry.

Magnetic field ψ, which is applied to the anisotropic object, produces torque if there is an angle difference between the *d*-axis and the field ($\delta \neq 0$), or if the *d*-axis of object "a" is not aligned with the field [12].

In the SynRM field, ψ is produced by a sinusoidally distributed winding in a slotted stator, and it links the stator and rotor through a small airgap, exactly as in a traditional induction motor. The field is rotating at synchronous speed, ω_s, and can be assumed to have a sinusoidal distribution. In this situation there will always be a torque, which acts to reduce the potential energy of the whole system by reducing the distortion field in the *q*-axis, ($\delta \rightarrow 0$). If δ, the load angle, is kept constant, then electromagnetic energy will be continuously converted into mechanical energy.

Therefore, the two most important parameters are: inductances L_d and L_q of the direct and quadrature axes , respectively. The power of a synchronous reluctance machine is obtained from the load angle equation (2.1) [13].

$$P = 3U_s^2 \frac{L_d - L_q}{2\omega_s L_d L_q} \sin 2\delta = \frac{3U_s^2}{2\omega_s} \left(\frac{1 - \frac{L_q}{L_d}}{L_q} \right) \sin 2\delta, \tag{2.1}$$

where

U_s – stator phase voltage;

L_d and L_q – d- and q-axis inductances;

δ – load angle;

ω_s – synchronous angular velocity,

In principle, the machine can yield its maximum torque at load angle $\delta = 45°$. Saturation and other phenomena may cause apparent deviation from this value [14].

2.2. Main Parameters and Design Limitations

Sizing is based on the in-production induction motor for the trolleybus application (made by AS "RER"). As SynRM was developed to replace IM, the casing size, electrical supply parameters, mechanical parameters, and construction possibilities of the manufacturer (airgap width δ) had to be considered.

The rated point for SynRM is chosen the same as for the induction motor, as it is well suited for the chosen traction characteristic. The rated point and sizing constraints are presented in Table 2.1.

Table 2.1

Rated Point and Sizing Limitations of SynRM

Parameter	**Unit**	**Value**
Rated output power	P_n [kW]	180
Rated voltage	U_n [V]	420
Rated frequency	f_1 [Hz]	50
Number of pole pairs		2
Number of phases		3
Operating regime		S2–60 min
Stator outer diameter	D_{os} [mm]	493
Stator stack length	L [mm]	290
Airgap width	δ [mm]	1.2

2.3. Stator Design

The stator was designed by performing calculations described in literature sources [15], [16], [13], and [17] with the addition of mathematical modelling of the magnetic field using the finite element modelling method (FEM).

2.4. Rotor Design

The rotor was designed by FEM magnetic field modelling for various rotor models. Important parameters were chosen from recommendations in the literature. The number of flux barriers and their positioning were chosen by the method described in [18] and [19]. The width of the rotor barriers and flux paths were chosen from recommendations in [20]. The designed rotor with the main geometrical parameters is presented in Fig. 2.2.

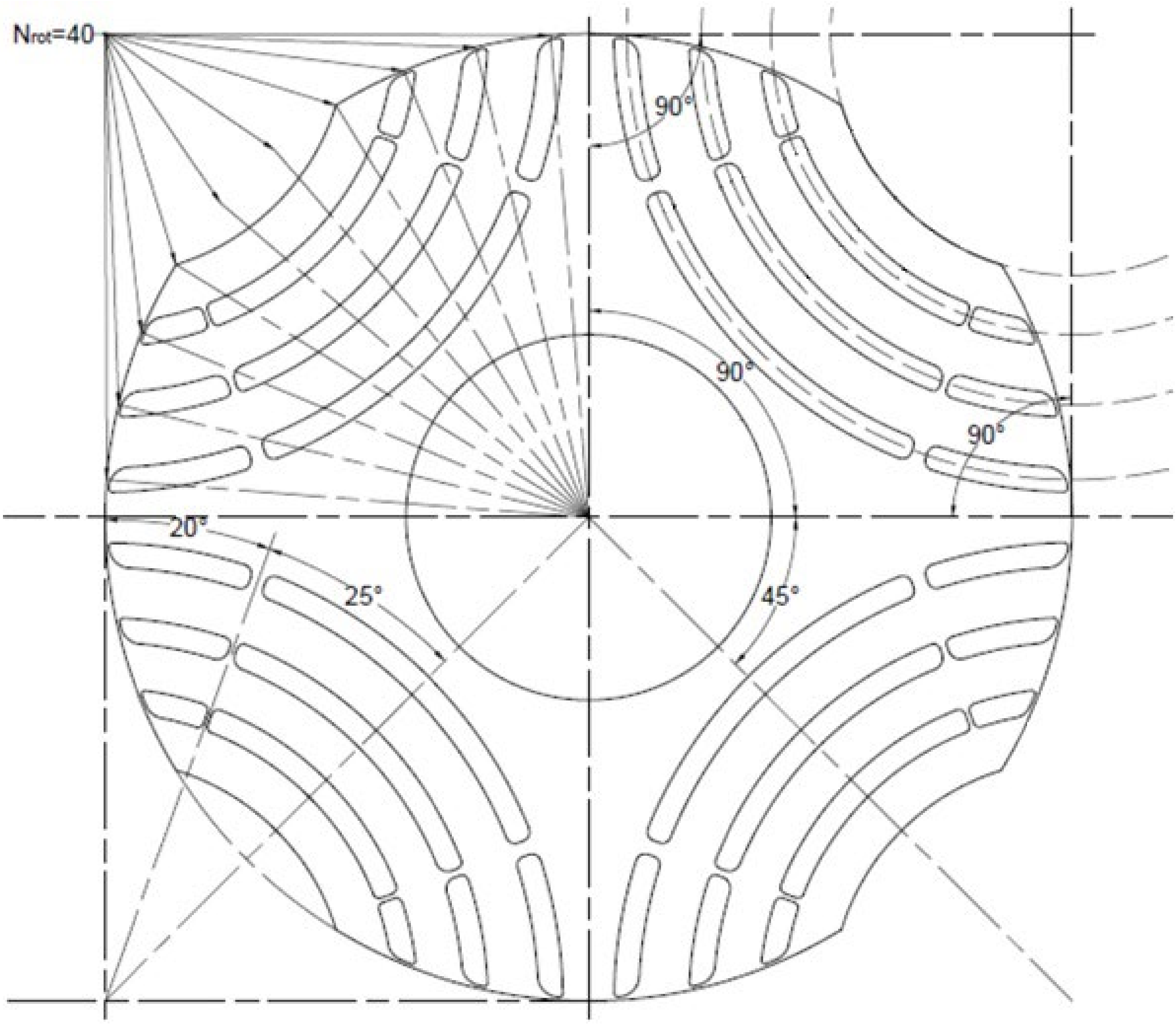

Fig. 2.2. SynRM rotor sheet geometry

2.5. Parameters of the Designed Motor

To evaluate the design process, losses were split into their components. Reported values are at a constant 50 Hz frequency. Table 2.2 presents the comparison of the test results of the designed SynRM and IM.

Table 2.2

Comparison of SynRM (FEM Modelling) and IM Test Results

Parameter	Unit	Design	IM
Supply current	I_1 $[A]$	392.4	309
Supply voltage	U_1 $[A]$	420	420
Power factor	$\cos\varphi$	0.663	0.85
Supply power	P_{in} [W]	189200	191400
Mechanical power	P_{out} [W]	179144	177989
Rotor angular velocity	n [RPM]	1500	1471
Mechanical torque	T_{out} [W]	1141	1156
Stator winding losses	ΔP_{el1} [W]	5637	5017
Rotor winding losses	ΔP_{el2} [W]	–	3580
Iron losses	ΔP_{mag} [W]	2873	1940
Mechanical losses	ΔP_{mech} [W]	544	960
Additional load losses	ΔP_{add} [W]	1002	1914
Total losses	$\Sigma\Delta P$ [W]	10056	13411
Efficiency	η [%]	94.69	92.99

SynRM power factor (0.663) is low compared to IM (0.89), consequently the current is higher. When designing SynRM, a trade-off between the power factor and torque capacity is unavoidable. The primary goal of the research was to obtain the required torque and efficiency reducing possibility for power factor optimization.

2.6. Traction Characteristic of the Designed Motor

Designing of the motor is followed by the calculation of parameters at different operation points, to see whether the designed motor is capable to either produce required reference torque or accelerate the trolleybus in required time.

Therefore, an algorithm is developed to calculate the parameters of Synchronous Reluctance Machine (SynRM) and to construct motor characteristics, considering the cross magnetic saturation effect. The algorithm includes a numerical calculation part and an FEM part. FEM is performed by defining three-phase currents in winding and solving the magnetostatics model.

The algorithm is designed for the machine mode at sinusoidal AC voltage, although in practice the SynRM is almost always coupled with a drive. Motor design calculations are usually made on the assumption that the operation is provided by a sinusoidal AC voltage [15]. The developed algorithm differs from the Kamper method [21] in that the reluctances are determined by calculating the electromagnetic torque by the FEM, and according to the vector diagram of SynRM, the reluctances of the armature direct axis and quadrature axis are determined. Similar algorithm for the induction machine mode determination that involves FEM calculations for the reactance computation with the voltage and the phase angle as the end criteria is presented in [22]. the developed method and calculation steps are described in more detail in publication [23].

In outline, the algorithm has *d*- and *q*-axis currents and field frequency (rotational speed) as inputs from which other parameters are iteratively calculated up to specific accuracy. Input currents are adjusted to stay within the voltage limit.

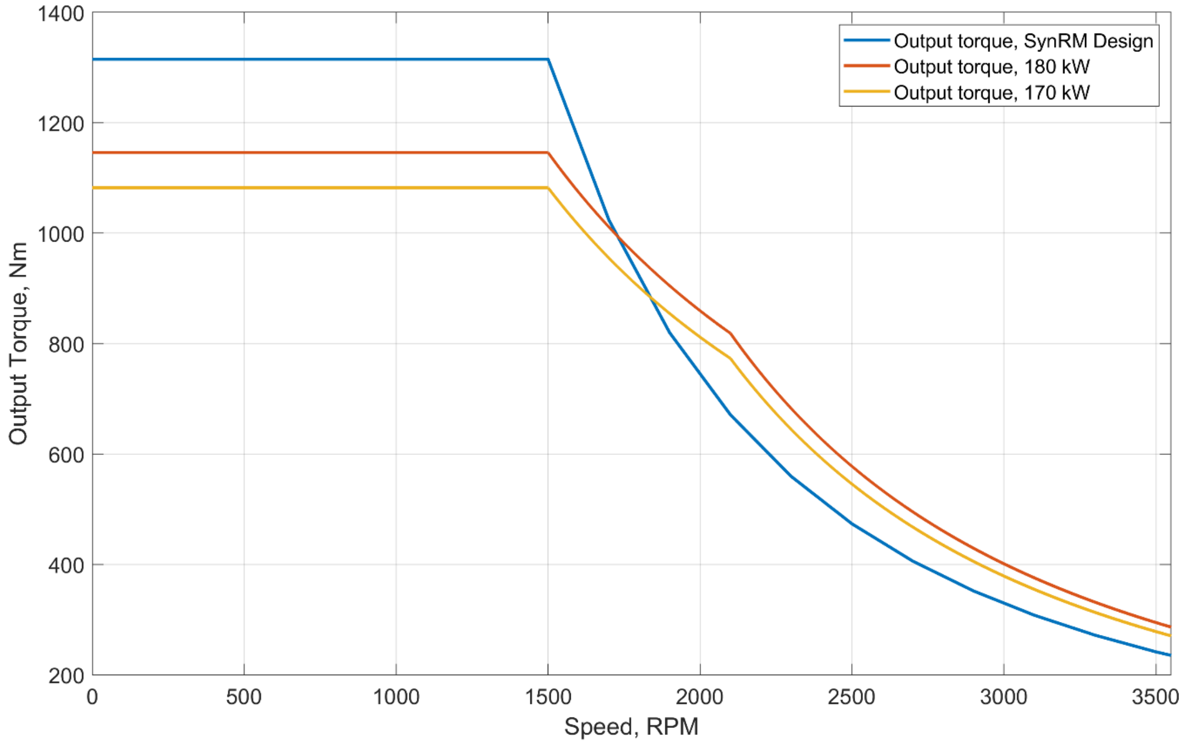

Fig. 2.3. Traction characteristic of the designed SynRM.

After the calculations, traction characteristic is obtained from 20 Hz (600 RPM) up to 120 Hz (3600 RPM, which corresponds to 65 km/h) with maximum obtainable torque limited by the rated voltage of 420 V. Figure 2.3 presents the traction characteristic with the designed SynRM and reference curves for reference.

3. Development of Control Algorithm and Model

Electric drive performance and robustness is vitally dependent on the control system. Due to the reluctance nature of the produced torque, SynRM has highly nonlinear characteristics, therefore design of its control algorithm is a challenging issue. The developed control system is based on fundamental SynRM equations, which were introduced in field-oriented control algorithm. Matlab Simulink model was created for verification of the control system.

This chapter describes the mathematical model of SynRM, control approach for SynRM, and modelling of the control system in Simulink.

3.1. Mathematical Model of SynRM

Inherently SynRM cannot be operated without inverter, and primarily two control methods are used for precise control: field-oriented control and direct torque control. Both approaches provide separate control of motor magnetisation and torque. These methods rely on mathematical models of the motor in rotating reference frame. The following equations is a commonly used mathematical model of the motor [24]:

$$\begin{aligned} v_d &= R_s i_{ds} - \omega_s L_q i_{qm} + L_d \frac{di_{dm}}{dt}, \\ v_q &= R_s i_{qs} + \omega_s L_d i_{dm} + L_q \frac{di_{qm}}{dt}, \end{aligned} \tag{3.1}$$

where i_{ds} and i_{qs} are stator current *d*- and *q*-axis components and R_s is stator winding resistance.

The mathematical model is derived from the equivalent circuit representation of SynRM shown in Fig. 3.1 with the vector diagram of SynRM at steady-state in Fig. 3.2 [12].

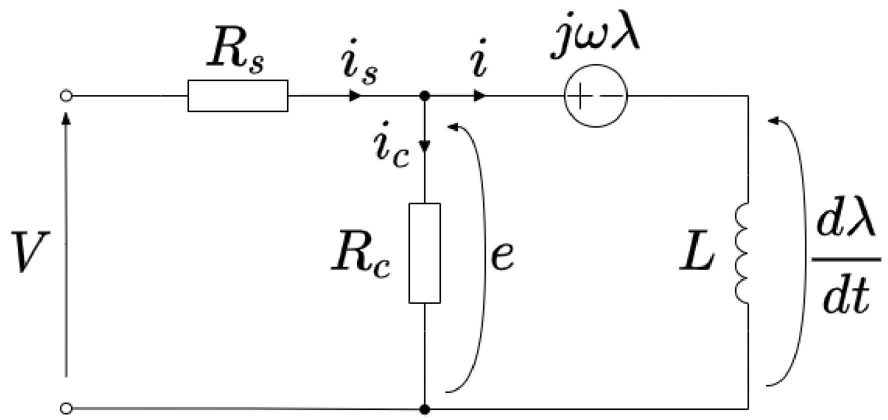

Fig. 3.1. SynRM equivalent circuit including iron loss.

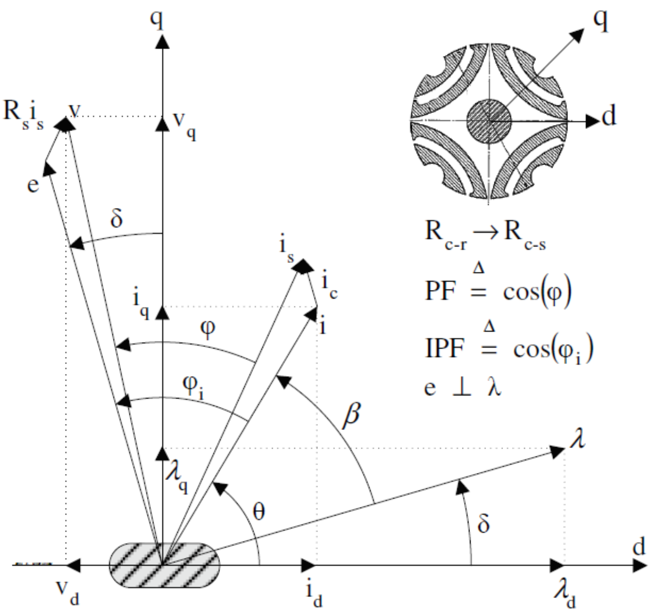

Fig. 3.2. Vector diagram of SynRM at steady state, where δ is load angle, θ is current angle, β is the torque angle, and φ and φ_i are the angles corresponding to power factor and internal power factor, respectively.

Power factor and internal power factor angles differ due iron and copper losses.

3.2. Implementation of Embedded Motor Control

The motor control system was developed on a control board with MCU TI TMS320F28335. The control unit was specially designed for an inverter with DC link voltage up to 1 kV and rated power up to 350 kW. The switching frequency of the inverter is 2 kHz.

The structure of the control system is shown in Fig. 3.3. The MCU receives 7 analog current signals, one analog voltage signal and an encoder signal from speed sensor. The IGBTs control signals are generated by the ePWM module. The IGBTs driver error signals are connected to the EPWM TZ module for fast response. The SPI serial communication peripherals are configured to communicate with the resolver readout board. The CAN module is responsible for data exchange (receiving commands and transmitting data) with the control computer.

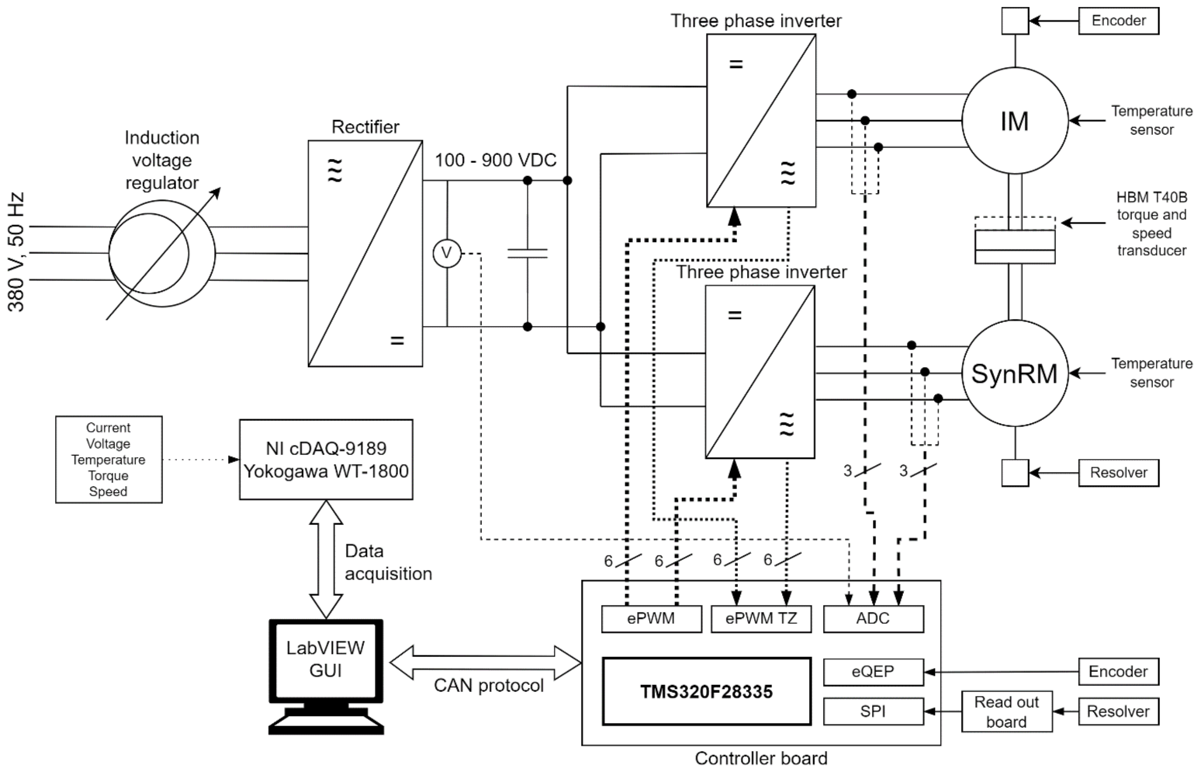

Fig. 3.3. The structure of the control system.

The built-in converter control software is written in Embedded C. Functions from the TI Digital Motor Control [25] library were used as fundamental mathematical blocks to form the motor control code. During the project, the functions were modified to adapt to the specific application.

3.3. SynRM Control Algorithm

Modern AC motors rely on the frequency converters with direct torque control or vector control, especially in traction application. In this research the field-oriented control (vector control) is used.

Frequency converters of SynRM drives make it possible to use a rotor with flux guiding barriers for efficient synchronous operation. The rotor enables a higher saliency ratio, which improves efficiency of the machine and reduces inertia. Lower inertia improves transient response time. The SynRM stator is identical to that of an asynchronous machine, and its control system comprises similar components.

Vector control technique requires usage of the two-axis model of SynRM in the rotor reference frame. It is achieved by *dq*-transformations of stator currents using rotor angle information, such as position or speed feedback. In case of synchronous motors, resolver is the most convenient option.

These control strategies rely on the control of current angle θ, and the appropriate current angle is chosen based on the desired performance [14], [12].

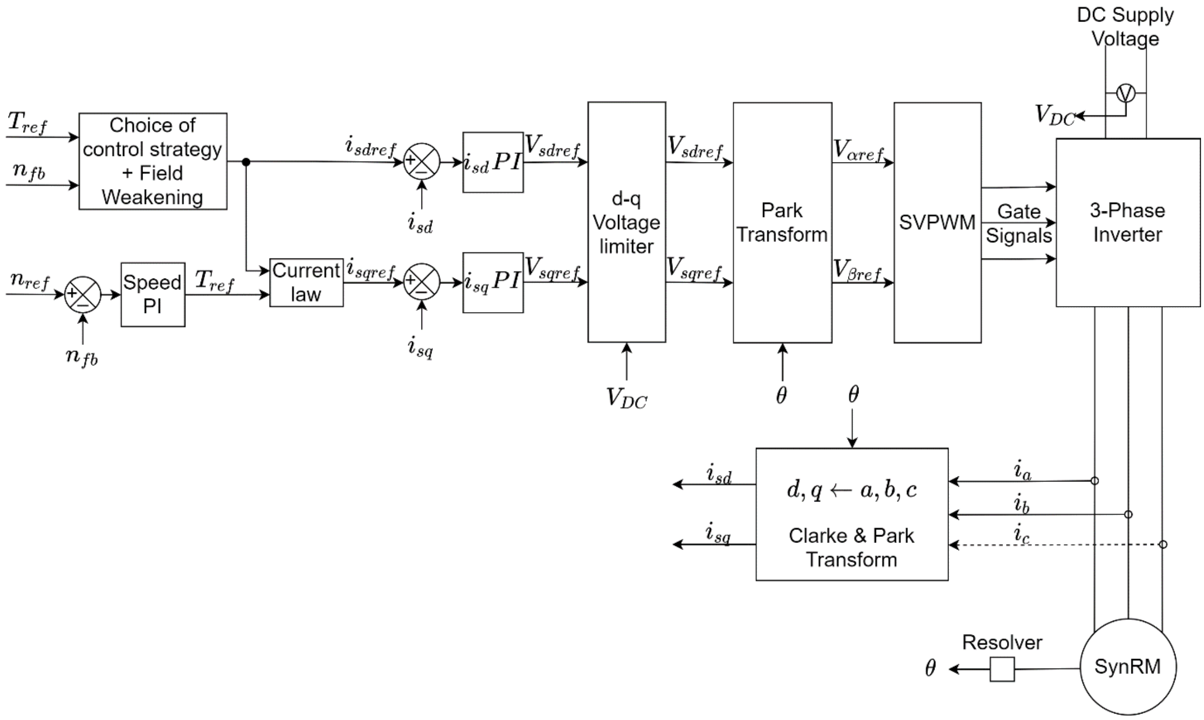

Fig. 3.4. Schematic block diagram of the vector control system for SynRM.

Figure 3.4 presents the general view of the vector control approach for SynRM, where torque control block could implement different approaches listed further.

The most used approaches to the vector control of SynRM are [26]:

- constant d-axis current control (CDAC);
- maximum rate of change of torque (MRCT);
- maximum power factor control (MPFC);
- maximum torque per ampere control (MTPA).

3.4. Simulink Model of the Electric Drive

The first step of verification of the control system before it is used on real setup is testing with a mathematical model. Moreover, modelling could help to investigate the edge cases of operation and is able to test the drive connected to the vehicle, which is usually not achievable in the laboratory test-bench setup.

The mathematical model of the SynRM electric drive of the trolleybus is created in Matlab Simulink environment. The model is a continuation of work presented in conference paper [27].

3.4.1. High-level Overview of Algorithm

Understanding of the inner workings of the Simulink model of the SynRM electric drive requires an overview of the logical connections and signal routes on the top level. The high-level overview is shown in Fig. 3.5.

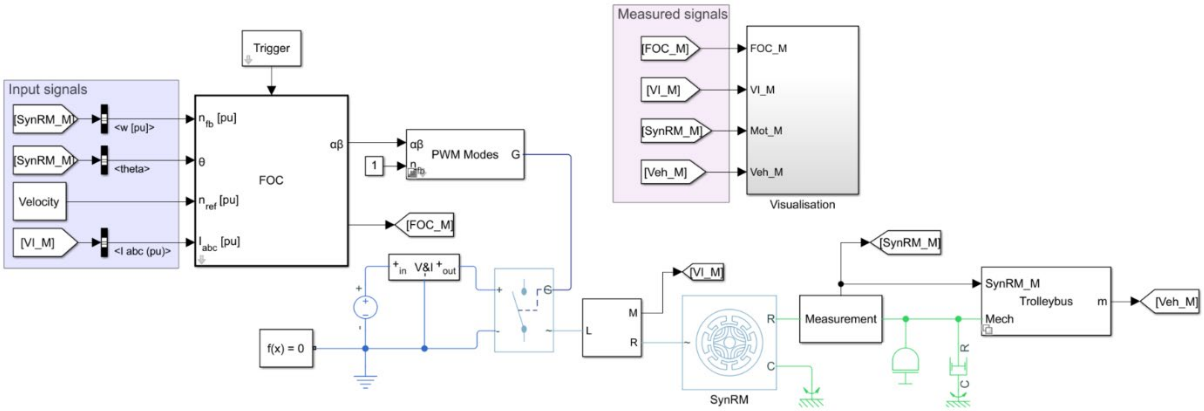

Fig. 3.5. High-level overview of electric drive model.

At the system start-up, the model is initialised with the script containing constants and look-up tables for proper operation. The used values are obtained based on the knowledge of SynRM, vehicle, and the test-bench setup. Furthermore, at the start-up, the motor connection could be switched between the test-bench operation (constant load in N·m) and vehicle connection.

The top-level model is organised into several subsystems or sections. Those are field-oriented controller (FOC), PWM generation for the inverter (supports several modulation approaches), traction inverter with DC voltage source, stator current and voltage measurement block, SynRM, rotor shaft measurements (rotor positions, output torque, rotor speed), and load subsystem. The load subsystem can be switched between the connection to the constant torque and vehicle.

Reference speed could be set as any speed as a function of time. For road profile testing, WLTP Class 1 is used.

3.4.2. Mathematical Model of the Trolleybus

Significant difference from the laboratory test-bench setup is the presence of the vehicle model, which in this case is the trolleybus. The model is based on the linear model of a moving object. The overview of the trolleybus model is shown in Fig. 3.6.

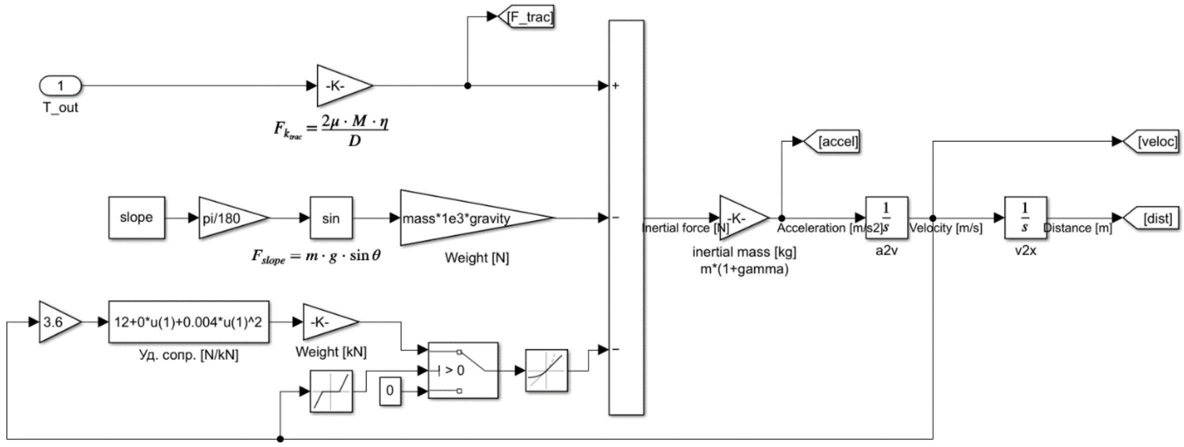

Fig. 3.6. Overview of the trolleybus model.

From the viewpoint of dynamics, forces acting on a vehicle in motion are determined by the Newton's Second law and could be represented as shown in Fig. 3.7 [28].

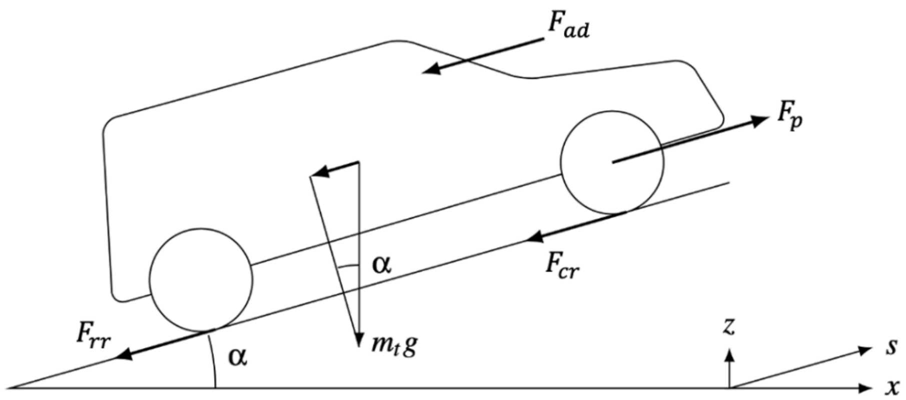

Fig. 3.7. Representation of forces acting on a vehicle in motion,

where F_{ad} is air-drag force [N]; F_{cr} is cornering resistance force [N]; F_{rr} is rolling resistance force [N]; α is the slope of the surface [‰]; and m_t is total effective vehicle mass [kg].

The total effective mass of the vehicle differs from the actual mass by correcting coefficient $1 + \gamma$, and it represents the effect of total inertia of rotating parts. This coefficient could be obtained by estimation through tests, or by calculations knowing the vehicle structure. For the trolleybus, the correcting coefficient for inertial mass is estimated to be 0.15–0.20 [29] (in the model 0.17 is used).

Air-drag, rolling resistance, and cornering resistance have their corresponding estimative formulas, but as they are describing complex physical phenomena, it makes them difficult to estimate. In practical calculations empirically obtained dependencies are usually used to describe these forces.

Such dependency is obtained by getting vehicle up to speed, then letting it coast on a flat long straight road, with no wind. In this test deceleration is observed, and then, this speed variation is expressed using a second order polynomial to approximate the effects of these resistance forces acting on a vehicle. General approximation is shown in the following equation [28], [29], [30]:

$$F_{res}(t) = C_0 + C_1 v(t) + C_2 v(t)^2. \tag{3.2}$$

In the case of this model, the equation from [29] and [30] is taken as an approximation:

$$w = 12 + 0.004 \cdot v^2; \tag{3.3}$$

$$F_{res} = w \cdot mg; \tag{3.4}$$

where v is km/h, and w is N/kN or a relative value per kN of force. To transform it to absolute values, it is multiplied by the weight of the vehicle.

4. Experimental Investigation of SynRM Traction Drive

The accuracy and quality of the production of an electric machine is reflected in its parameters and the convergence of the results of modelling and testing. An important stage of the research is the correction of the mathematical model of the electric motor according to the test results.

This chapter describes the production process of an electric machine, the laboratory and measuring instruments, and the test results.

4.1. Production Process of the SynRM Traction Drive

Production of the SynRM prototype was done at JSC "RER".

The motor consists of two main assembly units – stator and rotor.

Manufacturing of the stator of an electric motor begins with the motor housing. The housing of the SynRM prototype is welded from the smaller assembly units. The housing consists of a shell, poles, two side plates, which are interconnected by two steel channels. These parts are welded together and machined for purpose. The poles are machined for the size of steel stator sheets, necks for the end shields, and a keyway is slotted to fix the stator steel sheets inside the housing.

Next, a core made of electrical steel sheets is pressed into the housing. The stator core is sandwiched between the housing collar and the segment keys welded to the outer stator ring.

After that, in the stator are placed copped coils, which are connected according to the electrical connection scheme from the design stage. Finally, the stator is impregnated with a special compound for structural integrity and insulation, then dried and prepared for assembly.

The rotor of SynRM is a steel shaft on which the rotor steel sheets are stacked. Since this motor is made as an experimental prototype, it was sensible to make the rotor and stator sheets by cutting them out on a laser and not to order expensive technological equipment in the form of stamps.

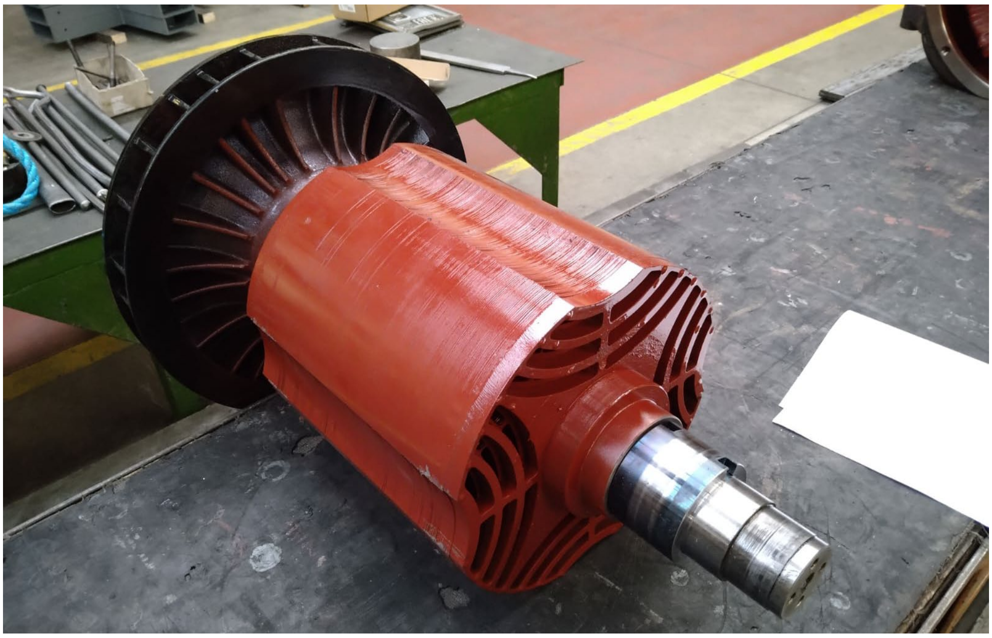

Fig. 4.1. Assembled rotor body.

After the stacking process, the rotor is impregnated in a similar process as a stator, machined (sanded), and then the fan is installed. At the final stage, the rotor is dynamically balanced. A completed painted rotor is shown in Fig. 4.1.

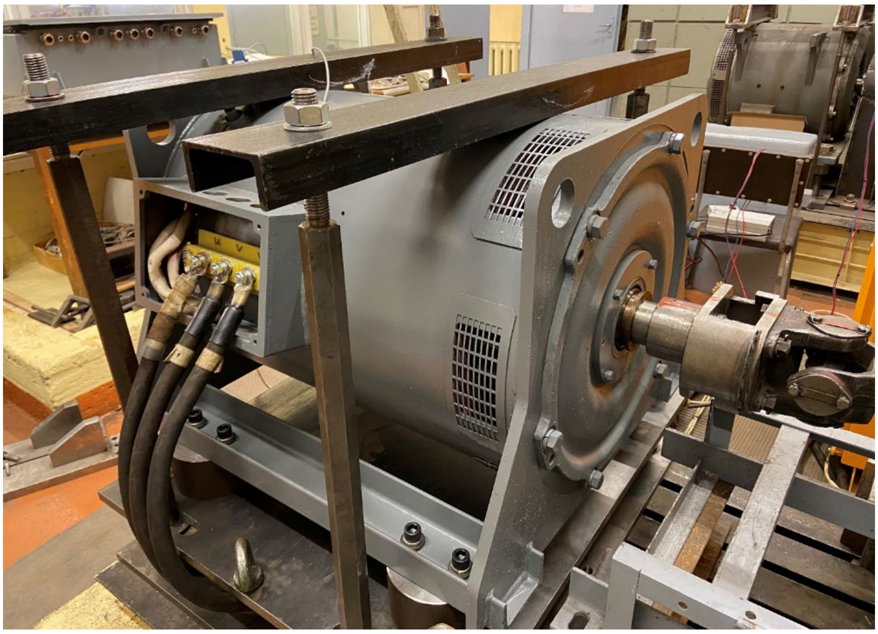

Fig. 4.2. SynRM traction drive on a test-bench.

SynRM that has been completed and installed on a test-bench is shown in Fig. 4.2.

4.2. Laboratory Testing of the Developed SynRM Traction Drive

Comprehensive laboratory testing of the designed and produced prototype is a crucial component in the research and development of the SynRM electric drive for the electric vehicle.

The tests of the manufactured sample were carried out in one of the traction laboratories of JSC "RER". The company is the largest manufacturer of electrical equipment for transport in the Baltics. The JSC "RER" development team implements various research results in the field of electric drives. The author participated in the tests of a dump truck electrical equipment set [31], as well as in studies on vibration of electric motors of electric trains [32], [33].

4.2.1. Laboratory Equipment

Testing Setup

Laboratory testing of the produced SynRM prototype requires a laboratory test-bench with the corresponding measurement and control equipment.

Laboratory tests were conducted at the test-bench setup of laboratory of urban vehicle electric drives up to 1kV DC at the premises of JSC "RER" [27]. The test-bench setup is shown in Fig. 4.3, and the inverter control board is shown in Fig. 4.4.

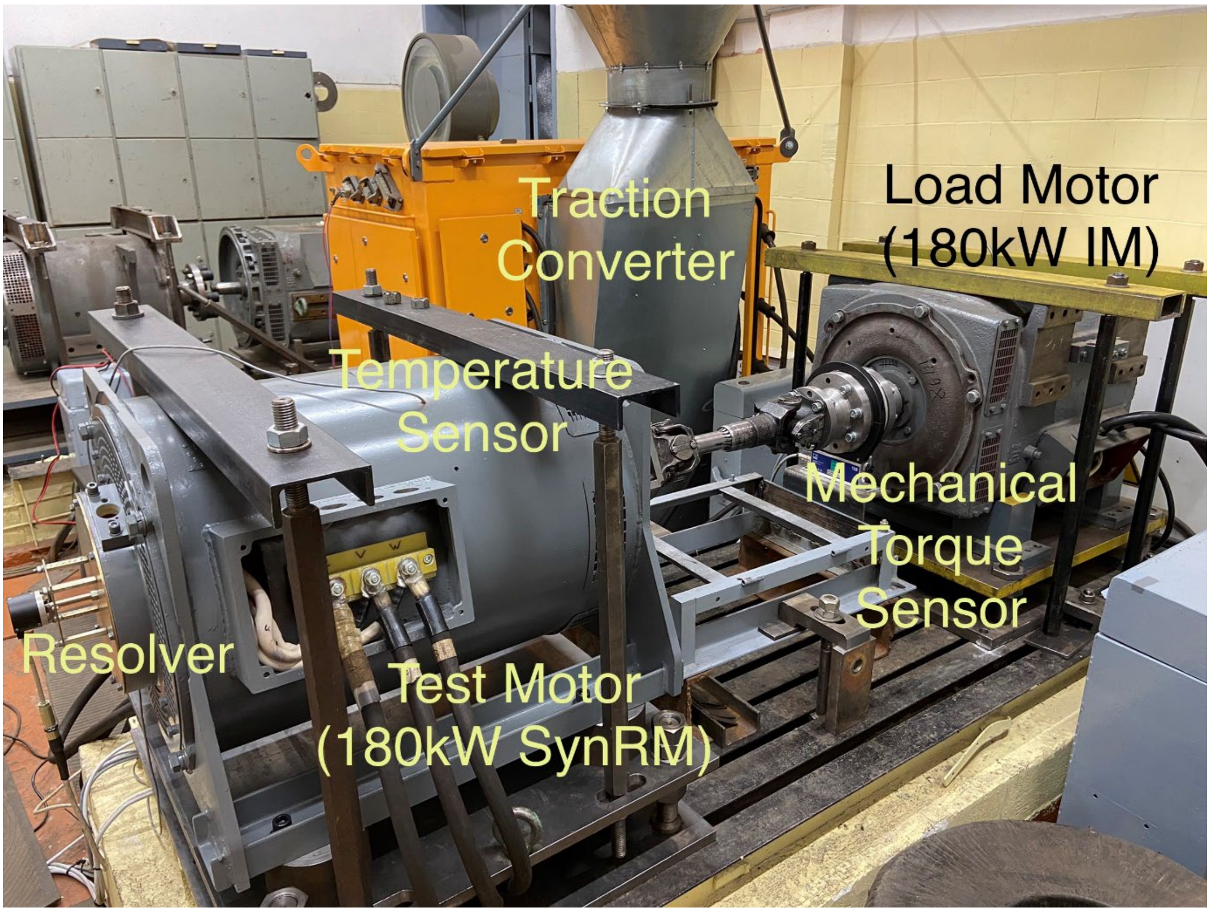

Fig. 4.3. Laboratory test-bench setup.

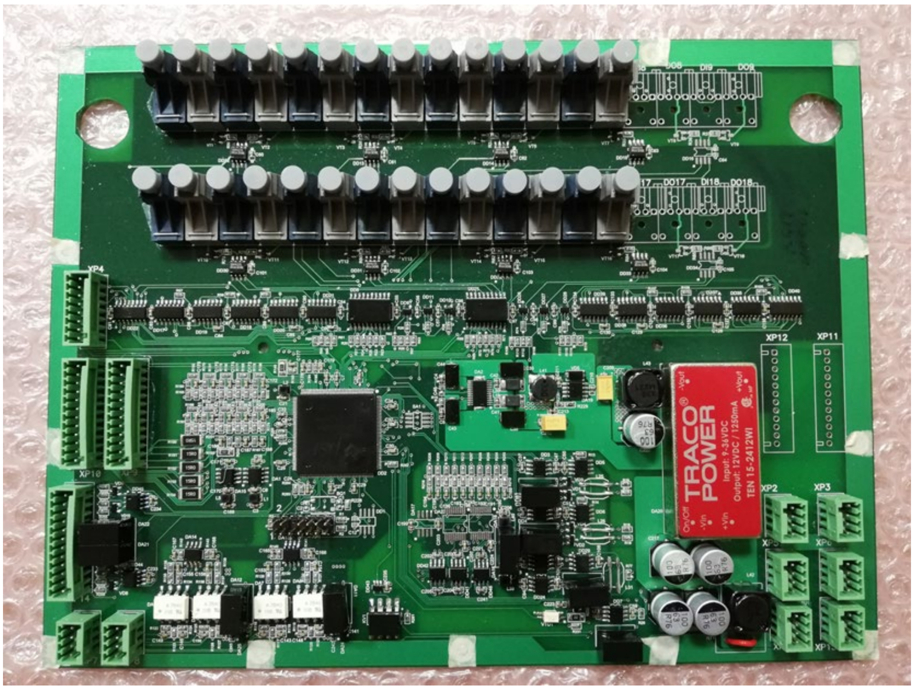

Fig. 4.4. Laboratory inverter control board MCU TI TMS320F28335.

Test and load motors are rigidly connected using a cardan joint and are mutually loaded. The motors are controlled by the traction converter supplied by the controlled DC-link voltage of up to 1kV. The control system is deployed to the TMS320F28335 digital signal processor (DSP). Control of the motors relies on the signals from the current and voltage sensors, from the resolver (rotor position sensor) for SynRM, and speed sensor for induction motor. Setting of reference parameters to the control system in the laboratory is done in graphical user interface (GUI), and communication with DSP is done using CAN bus.

Measurement Equipment

Besides the laboratory test-bench, there is a measurement and data analysis setup that allows to obtain, visualize and save all the data needed for research. Therefore, the quality of control and measurement results are approved by verified sensors and measuring equipment.

Output torque and rotational speed are measured using T40B 5kN·m torque transducer by HBM. Current values are measured by ES2000 hall sensors by ABB. Voltage is measured directly with Yokogawa WT1800 Precision Power Analyzer.

Data pre-processing and logging from the torque flange and temperature sensor are recorded using NI measurement setup. NI cDAQ-9189 chassis is used with NI9361, NI9215 and NI9216 modules, and the chassis is connected to the operating PC with the Ethernet connection.

4.2.2. Traction Characteristic of SynRM

Proper testing of the designed and produced SynRM is done to determine its tractive limitations, at and below 420 V at different speeds.

Rated Point Comparison

The designed motor and produced motor are compared at the rated point for the correspondence with each other at different parameters.

Table 4.1 presents the comparison at rated point (1500 RPM) and the rated output power (180 kW) of the designed motor. It shows that the efficiency of the design and prototype is very similar, while power factor is lower, leading to increase in required stator current. Additionally, magnetising current i_d is lower in the prototype to achieve the same value of supply voltage, meaning that inductances of the machine are slightly different.

Table 4.1

Comparison of designed and prototype SynRM at rated point

Parameter	**Unit**	**Design**	**Prototype**
Supply current	I_1 [A]	392.4	374.6
Supply voltage	U_1 [A]	420	417.1
Power factor	$\cos\varphi$	0.663	0.699
Supply power	P_{in} [W]	189200	189034
Mechanical power	P_{out} [W]	179144	179546
Rotor angular velocity	n [RPM]	1500	1498
Mechanical torque	T_{out} [W]	1141	1144.8
Stator winding losses	ΔP_{el1} [W]	5637	4409
Iron losses	ΔP_{mag} [W]	2873	2390
Mechanical losses	ΔP_{mech} [W]	544	810
Additional load losses	ΔP_{add} [W]	1002	1890
Total losses	$\Sigma\Delta P$ [W]	*10056*	*9488*
Efficiency	η [%]	94.69	94.99
d-axis current	i_d [A]	205.8	180.5
q-axis current	i_q [A]	526	501

Traction Characteristic

The produced SynRM was tested below 1500 RPM for required and slightly higher torque, while above 1500 RPM it was tested at 420 V up to the maximum achievable torque.

Figure 4.5 presents the traction characteristic comparison of designed, produced and reference torque characteristics.

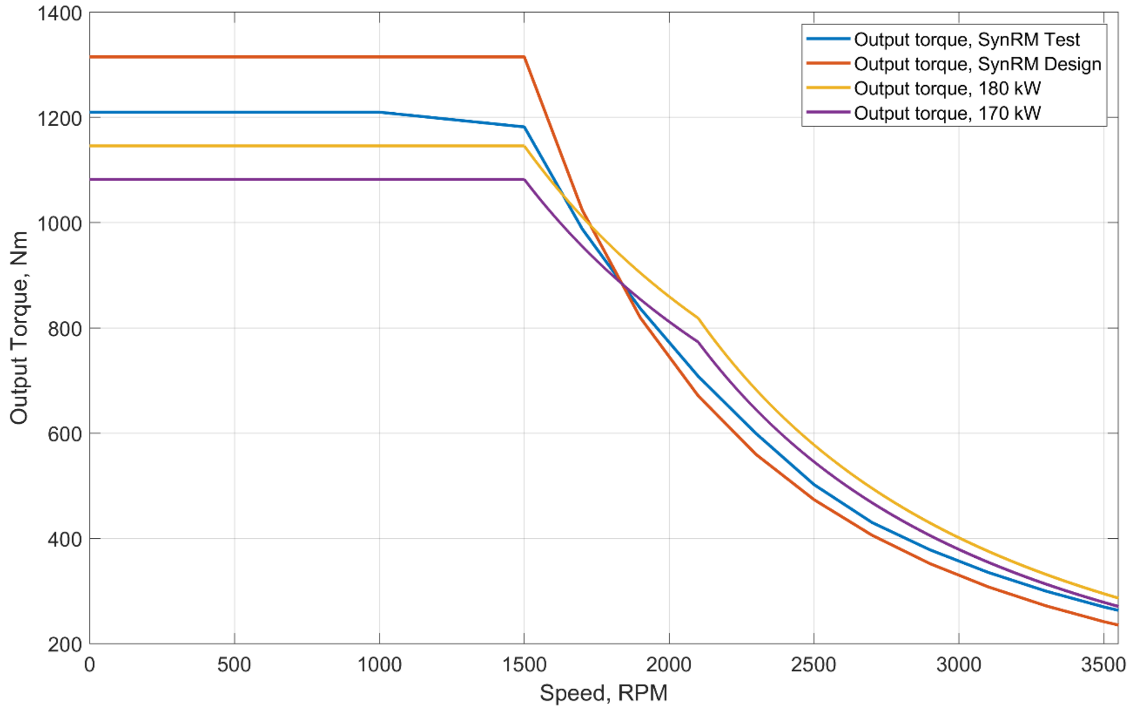

Fig. 4.5. SynRM test, design, and reference output torque curves.

Table 4.2 is the comparison of trolleybus performance of designed and produced performance

Table 4.2

Comparison of Trolleybus Performance with Designed and Produced SynRM

	Designed SynRM	Produced SynRM
	Horizontal road	
Time to 45 km/h, s	17.36	17.32
a_{max} $[\mathrm{m/s^2}]$	1.19	1.09
Residual force at 60 km/h	3.7 %	16.8 %
Top speed, km/h	60.7	63.1
	12 ‰ Inclination	
Time to 45 km/h, s	21.98	21.37
a_{max} $[\mathrm{m/s^2}]$	1.09	0.99
Residual force at 54 km/h	–	6.0 %
Top speed, km/h	52.9	54.8

4.3. D and Q axis Inductances

The most important values for the control and modelling of SynRM are d- and q-axis inductances (L_d and L_q correspondingly). For many mathematical models, parameters at rated point are sufficient, but for traction applications, it is crucial to know values at all points of inside traction characteristic, and/or inside torque limit at specified voltage.

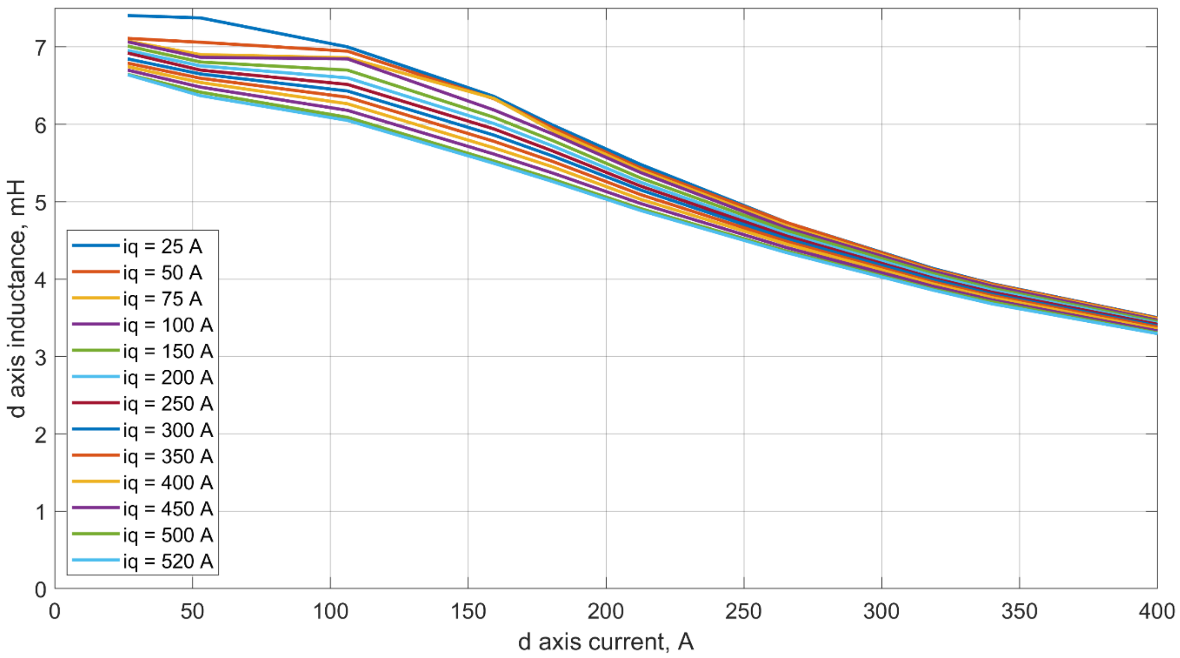

Fig. 4.6. D-axis inductance curve.

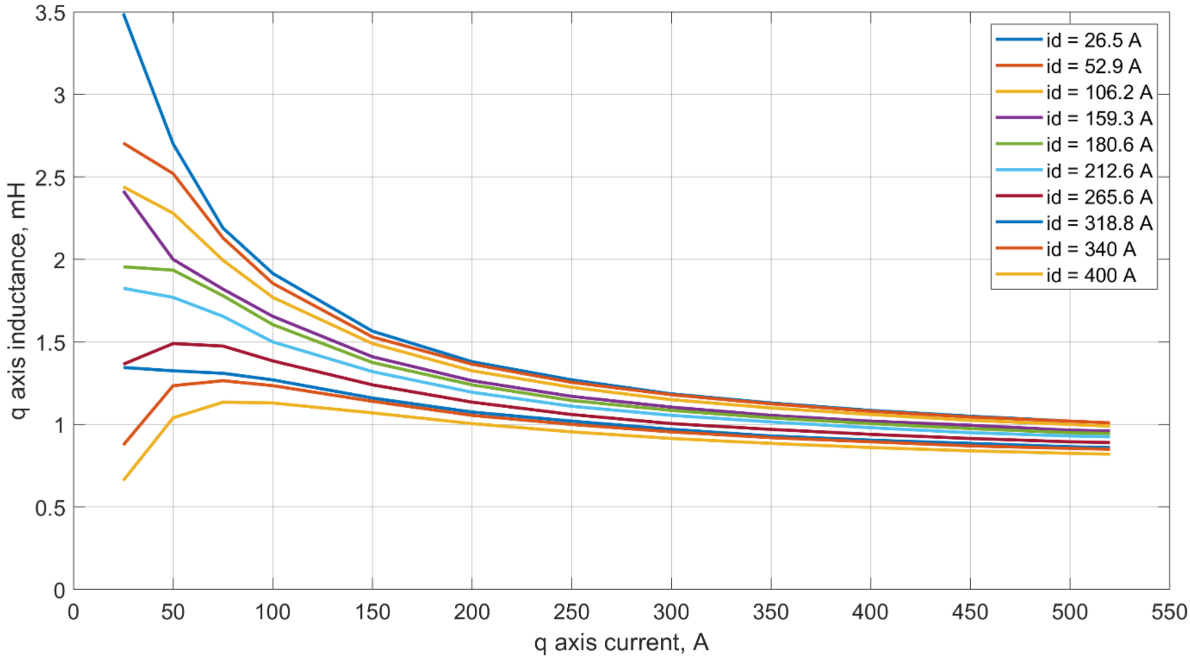

Fig. 4.7. Q-axis inductance curve.

It is very important to obtain accurate L_d and L_q values and their dependence on magnetic saturation and cross-saturation. Testing shows the dependency on both currents in a form of $L_d = f(i_d, i_q)$ and $L_q = f(i_d, i_q)$. L_d and L_q dependencies are shown in Figs. 4.6 and 4.7.

5. Verification of SynRM Control System Performance in Traction Drive

Verification of the control system performance allows to make conclusions about the developed product and provides information for future improvements. Verification is carried out by laboratory and model testing in different steady-state and transient regimes. Model testing allows to predict the control system performance on real vehicle in the edge cases, to assure stable operation. The performance of SynRM traction drive is also compared to the conventional IM traction drive.

5.1. Investigation of SynRM and IM Performance in Traction

5.1.1. Comparison of Maximum Torque Capabilities

The maximum torque coefficient indicates the ability of the electric motor to deliver the required torque at a reduced supply voltage. In vehicles powered by a DC traction grid, this indicator is critically important, since the grid voltage can be reduced by 30 % of the rated during operation.

Figure 5.1 shows the rated reference and theoretical maximum traction characteristics of the used 180 kW induction motor for the trolleybus. It could be seen that the maximum torque is significantly higher than the maximum torque of SynRM. In addition, in the field-weakening regime, the induction motor can provide the required torque, with a 50 % reserve at the maximum required speed.

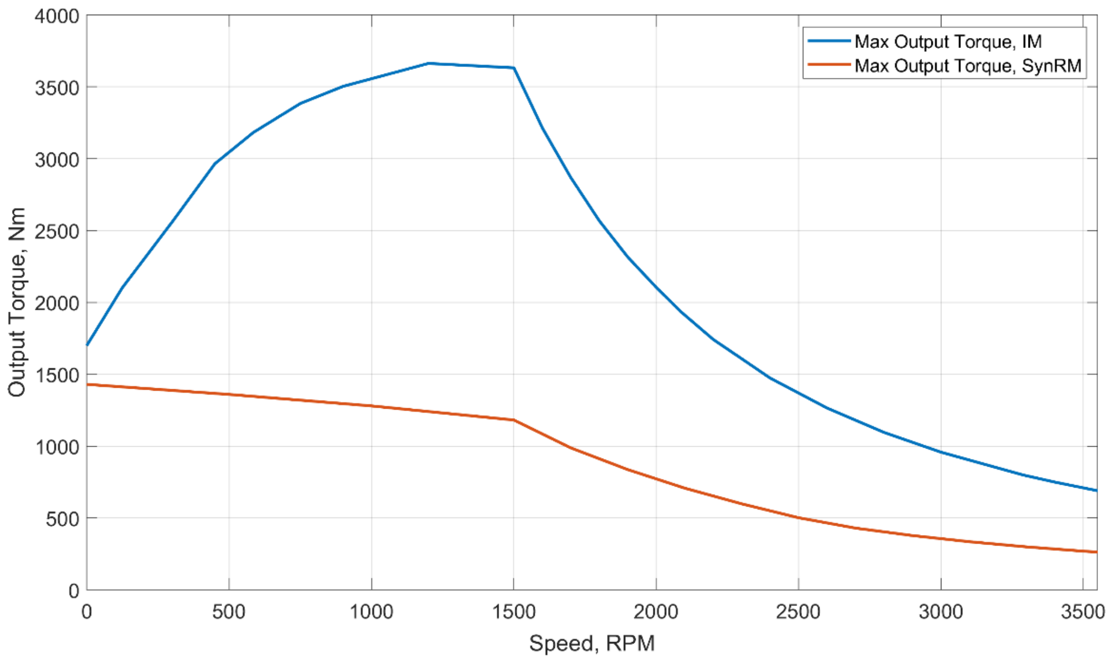

Fig. 5.1. Maximum output torque of 180 kW IM.

5.1.2. Comparison of Efficiency Indicators

For traction applications, it is convenient to use the efficiency map, since the motor operates in different modes. Full process description was published in the RTUCON 2021 Conference Proceedings [34].

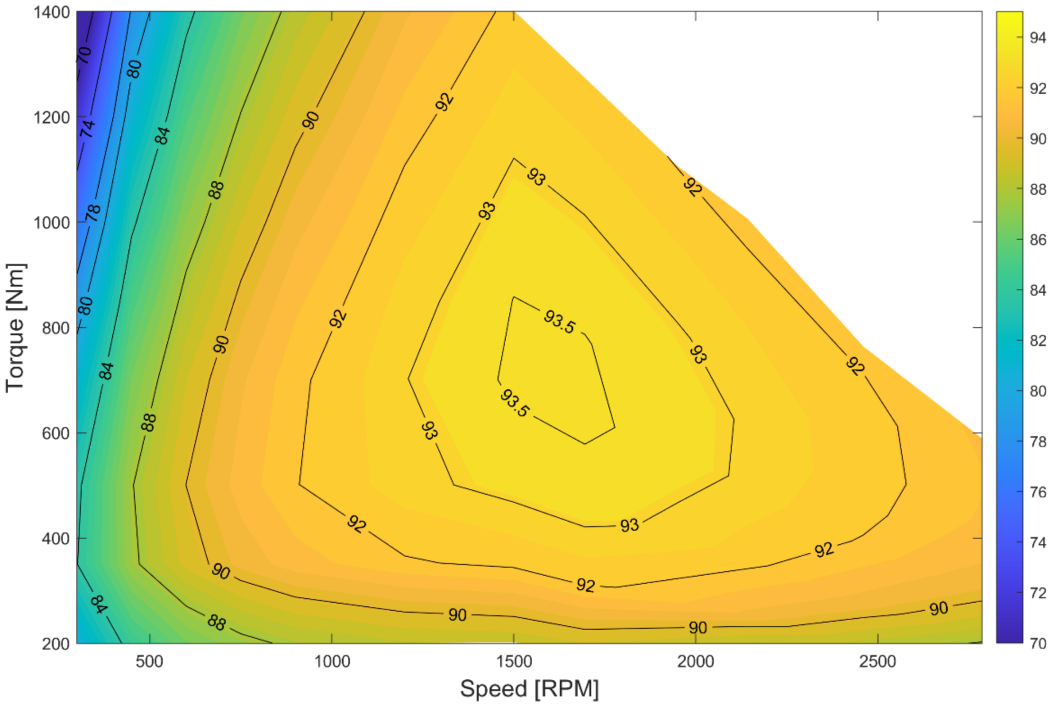

Fig. 5.2. Efficiency map of IM with $i_d = const.$

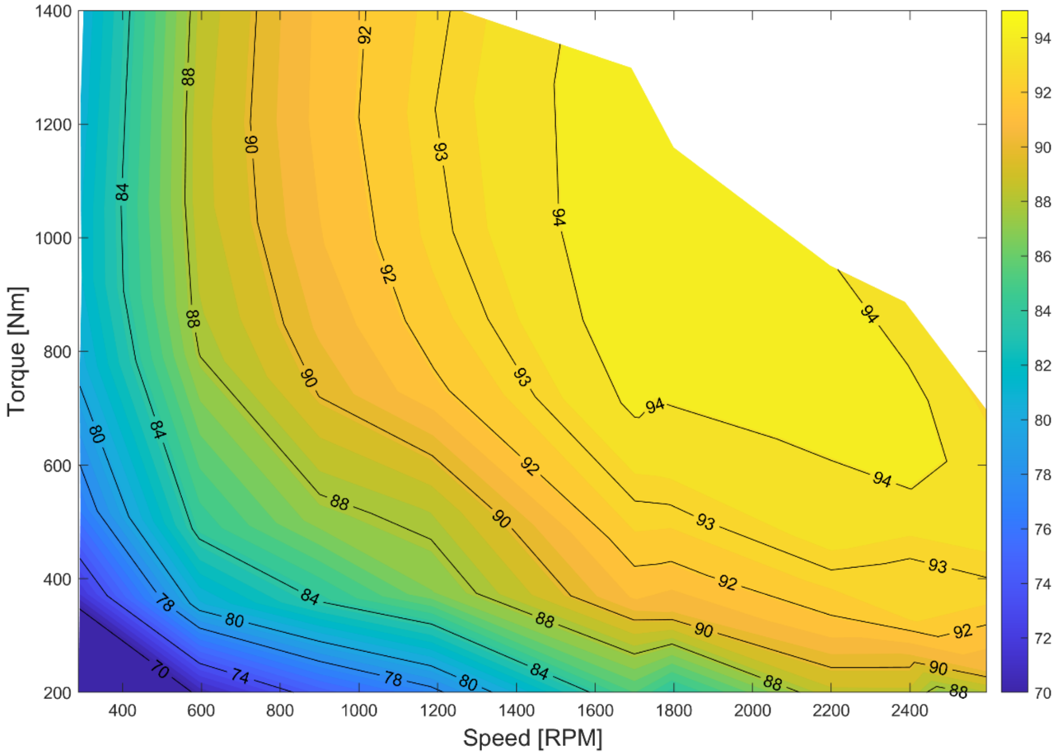

Fig. 5.3. Efficiency map of SynRM with $i_d = const.$

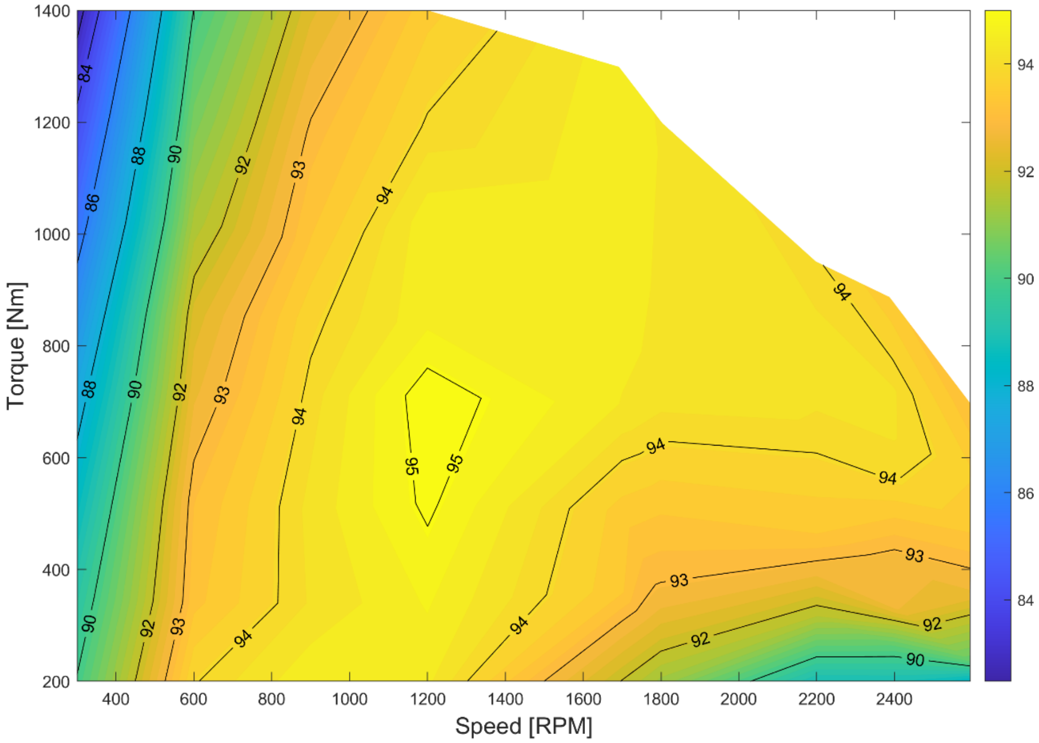

Fig. 5.4. Efficiency map of SynRM with MTPA

Initial comparison of IM and SynRM efficiency maps is done using the identical approach, i.e., with constant *d*-axis current control. This is done to compare the motors with the same control. The results are presented in Figs. 5.2 and 5.3. The tests were performed both below the rated point and above it in the field-weakening regime.

Figures 5.3 and 5.4 show the comparison of SynRM efficiency maps utilizing two different control strategies: constant d-axis current and MTPA controls. MTPA is used up to 520 V limit, which is the rated voltage of the machine. When the MTPA control becomes unachievable, it is switched to $i_d = const$.

It can be seen that at all operational points, where usage of MTPA is possible, efficiency of the machine is improved considerably. Moreover, the efficiency map of the SynRM with MTPA control is much flatter, with the minimum of 82.48 % at measured 300 RPM and 1400 N·m, and the maximum of 95.21 %. Whereas $i_d = const$ control falls to the minimum of 60 % at measured 300 RPM and 200 N·m, with the maximum of 94.71 %. In contrast, IM falls to 66.53 % at measured 300 RPM and 1400 N·m, with the maximum of 93.61 %.

5.1.3. Distribution of IM and SynRM Losses

More detailed information for thorough analysis of motors is obtained by means of distribution of losses with each of the control strategies. Summary of the rsults is presented in Table 5.1.

Table 5.1

Distribution of Motor Losses in Steady-State at Rated Point

Parameter	Unit	IM	SynRM CDAC	SynRM MTPA
Stator current	V	529	522	481.2
Stator current	A	229.4	370.5	350.6
Power factor		0.905	0.575	0.664
Input power	W	197276	193657	191451
Rotational speed	RPM	1500	1500	1500
Output power	W	180000	180000	180000
Output torque	N·m	1145.9	1145.9	1145.9
Stator Cu losses	W	4688	6176	5501
Rotor Cu losses	W	4055	-	-
Iron losses	W	5760	4863	3354
Additional losses (1 % of input power)	W	1973	1937	1915
Mechanical losses	W	800	681	681
Total losses	W	17276	13657	11451
Efficiency	%	91.24	92.95	94.02

5.1.4. Comparison of Power Factor

Power factor values have also been taken across the entire speed range. The power factor of IM is $\cos\varphi = 0.67 - 0.7$, and of SynRM it is $\cos\phi = 0.85 - 0.9$. This difference is based on the physical properties of the machine, and a lower power factor was expected at the design stage based on theoretical calculation.

5.1.5. Summary of the Comparison

Recently, many studies have been conducted comparing the characteristics of SynRM and IM [35], [36], [37]. However, in the mentioned studies, general industrial electric motors were used, and the issue of traction capabilities was not analysed. This research examines all the parameters required for traction applications.

After laboratory tests and comparative analysis, it could be concluded that the main advantage of the developed and produced synchronous-reluctance motor, compared to the induction motor, is efficiency. The efficiency of the developed motor is high, and its characteristic is much flatter not only at and near the rated point, but also in other regimes of operation.

On the other hand, the desire to increase efficiency negatively affected the torque margin of SynRM. To ensure the required torque, it was necessary to raise the magnetic induction in the iron, relative to the induction of IM, which is the main way of forming the torque in the SynRM. As a result, the SynRM provided the required torque up to rated speed but failed to meet the additional requirements for the traction application of electric motors. Insufficient torque margin degrades the dynamic performance of the vehicle in operation and leaves very low residual force at maximum speed.

Low power factor is another disadvantage of SynRM. The power factor does not affect the performance or efficiency of the motor but requires more current on the stator windings. As a result, it leads to increased losses in the frequency converter, as well as increases the requirements for the maximum current of the electric drive system. The disadvantage may be less important if the rest of the electric drive equipment has high efficiency.

5.2. Performance of the SynRM Traction Drive Simulink Model

For verification of Simulink model performance several tests were carried out. The trolleybus performance was evaluated based on dynamic requirements.

5.2.1. Acceleration to the Maximum Speed

The test for acceleration to the maximum speed is carried out to test the ability to hold the maximum traction characteristic and whether the fully loaded trolleybus can achieve the dynamic requirements. The speed reference is set to 60 km/h. Figure 5.5 presents the output characteristic during the test. It can be seen that acceleration to 45 km/h takes 17.15 seconds, which is inside of the maximum allowable time (Subchapter 1.1). Furthermore, the maximum speed of 60 km/h is successfully achieved with the residual force of 12.2 % ($T_{out\,max}$ at 60 km/h is 254 N·m, T_{out} at 60 km/h is 223 N·m).

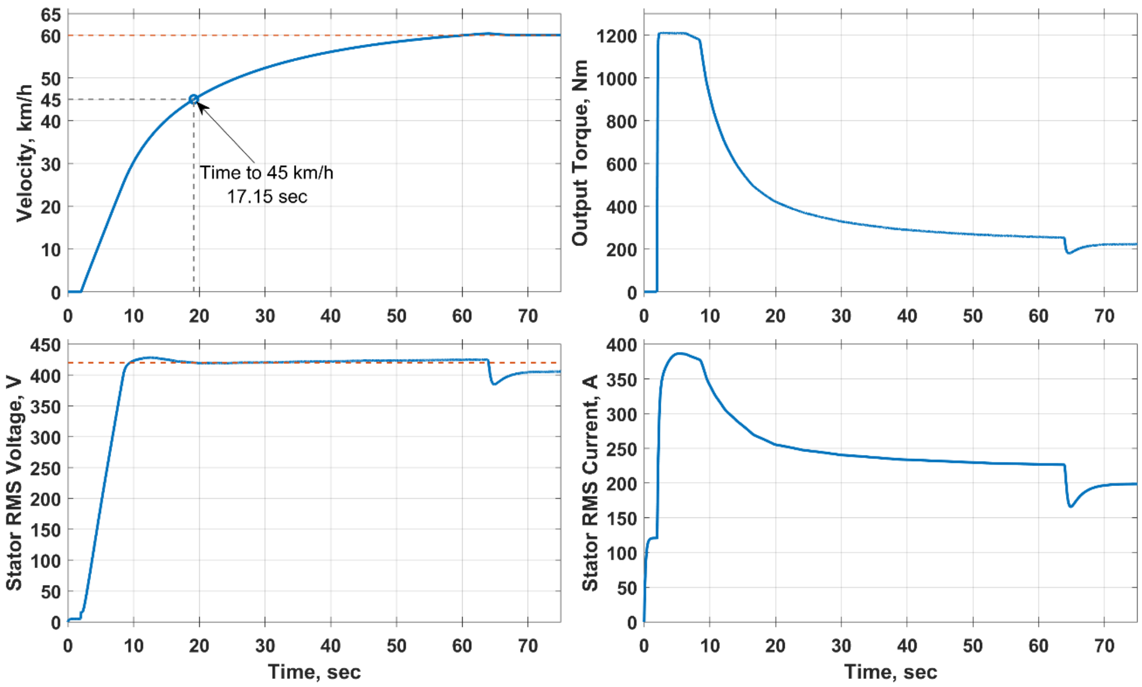

Fig. 5.5. Acceleration to maximum speed, output characteristics.

5.2.2. Performance of the Model

Performance of the Simulink traction drive model is tested with a standardized freely available road profile. For model testing the Worldwide Harmonized Light Vehicles Test Procedure defined by the United Nations Economic Commission for Europe [38] was chosen.

This test represents mixed use in an urban environment. Also, this test was selected because it is freely available for urban use, and trolleybus power to mass ratio is appropriate for the use with Class 1 [38].

Energy consumption

Table 5.2 shows the total energy consumed during the driving cycle in kWh. Braking energy is not accounted for recuperation and is just assumed to be converted to heat. Converter efficiency is set to $\eta_{conv} = 97.5$ %.

Table 5.2

Energy During WLTP Cycle

	Value [kWh]
Energy at the wheel	4.04
Input energy (SynRM CDAC)	4.69
Input energy (SynRM MTPA)	4.49
Input energy (IM CDAC)	4.67

From the results of total consumed energy, it can be seen that energy loss in the motor with the converter is 0.65 kWh for SynRM CDAC, while for the SynRM MTPA it is 0.45 kWh, meaning that 30.7 % reduction of motor loss could be achieved only with the control approach, with sustained level of dynamic performance.

The traction drive with the induction motor shows almost the same energy consumption as with CDAC SynRM (3.2 % more than with SynRM) and 40 % bigger energy loss difference compared to the SynRM with MTPA.

Conclusions

As a result of the project, an experimental prototype of the traction SynRM was developed in the dimensions of the existing IM. Firmware has been developed to control the drive. The operation of the control system was tested on a Matlab Simulink mathematical model. To confirm the results of calculations and simulations, laboratory tests were carried out.

Laboratory tests of SynRM showed a high convergence of the results with the calculated values at the rated speed. The main difference was in the stator current, which indicates a mismatch between the values of L_d and L_q at the rated speed. Determination of the inductance values is the most difficult design task, since it can strongly depend on the homogeneity and accuracy of the parameters of the magnetic circuit material, as well as on the quality of the motor assembly.

The torque limit values obtained during testing in the entire speed range also differ from the projected ones due to the discrepancies between the projected inductance curves $L_d(I_d)$ and $L_q(I_q)$ and the measured ones. The tests have shown lower values of the maximum torque at rated voltage, but higher in the field weakening mode. During laboratory tests the $L_d(I_d, I_q)$ and $L_q(I_d, I_q)$ curves were taken to correct the calculated coefficients. Further design iterations will be carried out, considering the specifics of materials and manufacturing deviations.

The SynRM control system was developed in the Matlab Simulink environment and tested on a real laboratory inverter. The field-oriented control (FOC) algorithm was adopted as a basis. The control system uses the instantaneous values of stator currents and the angle of the rotor position to form a reference of voltage values. To accurately determine the torque, the values of $L_d(I_d)$ and $L_q(I_q)$ were entered into the control system using look-up tables. Regulation of currents, torque and speed is carried out using PI controllers. During simulation and in laboratory conditions, the control system reliably and stably fulfilled the commands in the torque-control and the speed-control modes. The developed control system made it possible to implement all the planned tests necessary to confirm the operability and stability of the drive.

Simulation of the dynamics of the trolleybus movement with the developed SynRM showed that the drive meets the acceleration requirements when driving on a slope at rated voltage. The drive performs all specified accelerations and decelerations in the WLTP cycle. The disadvantage of this SynRM is a small margin for the maximum torque, which especially affects the performance of the drive when supply voltage drops below rated value. Even though, according to the requirements of the WLTP test cycle, the maximum torque is never reached, actual operation mode may be more severe.

When comparing SynRM and classic IM, the increase in efficiency declared during the design was confirmed during the tests. At the rated speed, the efficiency increased by 2 %. In a region below rated speed, the SynRM degrades the efficiency much more slowly than the IM efficiency. In turn, the power factor of SynRM is reduced relative to IM by 0.2, which increases the stator and inverter currents. When the efficiency of the inverter is high, the difference in power factor should not significantly affect the overall efficiency of the drive.

As a result of the research, it can be concluded that an electric drive based on SynRM can be an alternative to IM. However, in the initial design, it is important to consider the low critical torque reserve and low power factor.

List of References

[1] *WHITE PAPER Roadmap to a Single European Transport Area – Towards a competitive and resource efficient transport system, http://eur-lex.europa.eu/LexUriServ/LexUriServ.do?uri=COM:2011:0144:FIN:EN:PDF.,* 2011.

[2] J. Larminie and J. Lowry, Electric Vehicle Technology Explained, 2nd Edition, Wiley, 2012.

[3] "Possibilities of energy demand reduction in trolleybus transportation," CIVITAS, Brno, 2014.

[4] W. Backhaus, A. Bätzner, J. Kohout, E. Lenz, R. Kayser, and D. S. Röhlig, "Knowledge Brief, Infrasructure for In Motion Charging Trolleybus System," Knowledge Brief of UITP, the International Association of Public Transport, Brussels, July, 2021.

[5] R. R. Moghaddam, S. Nategh, J. Islam, and A. Boglietti, "Different Traction Motor Topologies Used in E-Mobility : Part II: Magnet-based Solutions," in *2020 International Conference on Electrical Machines (ICEM)*, 2020.

[6] E. Bostanci, M. Moallem, A. Parsapour, and B. Fahimi, "Opportunities and Challenges of Switched Reluctance Motor Drives for Electric Propulsion: A Comparative Study," *IEEE Transactions on Transportation Electrification,* vol. 3, no. 1, pp. 58–75, March 2017.

[7] Heidari, Hamidreza; Rassõlkin, Anton; Kallaste, Ants; Vaimann, Toomas; Andriushchenko, Ekaterina; Belahcen, Anouar; Lukichev, Dmitry, "A Review of Synchronous Reluctance Motor-Drive Advancements," *Sustainability,* 2021.

[8] J. K. Kostko, "Polyphase reaction synchronous motors," *Journal of the American Institute of Electrical Engineers,* vol. 42, no. 11, pp. 1162–1168, 1923.

[9] G. Abad, Power Electronics and Electric Drives for Traction Applications, Chichester: Wiley, 2017, p. 630.

[10] K. Gulbis, U. Brakanskis, E. Kamolins, M. Gorobecs, A. Potapovs, K. Sejejs, J. Zarembo and V. Burenin, "Analysis of Test Results of Developed Synchronous Reluctance Motor for Public Transport Application," *Latvian Journal of Physics and Technical Sciences,* 2021.

[11] A. Potapovs, U. Brakanskis, M. Gorobecs, K. Gulbis, E. Kamoliņš, K. Sejejs, V. Burenin, J. Zarembo, “180 kW Synchronous Reluctance Motor for Mass Transit Electrical Traction Application,” in *23rd European Conference on Power Electronics and Applications (EPE’21 ECCE Europe)*, Brussels, Belgium, 2021.

[12] R.-R. Moghaddam, Synchronous Reluctance Machine (SynRM) in Variable Speed Drives (VSD) Applications, Stockholm: The Royal Institute of Technology, 2011, p. 260.

[13] J. Pyrhonen, T. Jokinen and V. Hrabovcova, Design of Rotating Electrical Machines, Chichester: Wiley, 2014, p. 584.

[14] J. Pyrhonen, V. Hrabovcova and R. S. Semken, Electrical Machine Drives Control, Chichester: Wiley, 2016, p. 504.

[15] I. Boldea, Reluctance Synchronous Machines and Drives, Oxford: Clarendon Press, 1996.

[16] I. Boldea and S. A. Nasar, The Induction Machines Design Handbook, CRC Press, 2009.

[17] И. П. Копылов, Электрические Машины: Учебник для вузов, Москва: Энергоатомиздат, 1986.

[18] A. Vagati, M. Pastorelli, G. Franceschini, and S. C. Petrache, “Design of Low-Tourque-Ripple Synchronous Reluctance Motors,” *IEEE Transactions on Industry Applications,* vol. 34, no. 4, 1998.

[19] A. Vagati, “Synchronous Reluctance Electrical Motor Having A Low Tourque-Ripple Design”. Patent 5818140A, 6 October 1998.

[20] T. A. Lipo and T. Matsuo, “Rotor design optimization of synchronous Reluctance machine,” *IEEE Transaction on Energy Conversion,* vol. 9, no. 2, 1994.

[21] M. Kamper, A. F. Volsdhenk, “Effect of rotor dimensions and cross magnetisation on Ld and Lq inductances of reluctance synchronous machine with cageless flux barrier rotor,” in *IEEE Proceedings – Electric Power Applications, Volume 141, Issue 4*, July 1994.

[22] A. Podgornovs and R. Geidarovs, “Induction machine mode determination using vectograms and magnetic field calculation results,” in *2017 IEEE 58th*

International Scientific Conference on Power and Electrical Engineering of Riga Technical University (RTUCON), Riga, 2017.

[23] K. Gulbis, U. Brakanskis, E. Kamoliņš and J. Zarembo, “Parameter Calculation Method of Synchronous Reluctance Motor Including Cross Magnetic Saturation,” in *2020 IEEE 61th International Scientific Conference on Power and Electrical Engineering of Riga Technical University (RTUCON)*, Riga, Latvia, 2020.

[24] K. Yahia, D. Matos, J. O. Estima, and A. J. M. Card, “Modeling synchronous reluctance motors including saturation, iron losses and mechanical losses,” in *2014 International Symposium on Power Electronics, Electrical Drives, Automation and Motion*, Ischia, 2014.

[25] “Digital Motor Control. Software Library: Target Independent Math Blocks.,” Texas Instruments, Inc. C2000 Systems and Applications, 2013.

[26] A. J. P. Ortega, Design and Comparison of Induction Motor and Synchronous Reluctance Motor for Variable Speed Applications: Design Aided by Differential Evolution and Finite Element Analysis, The Ohio State University, 2013.

[27] V. Burenin, J. Zarembo, A. Žiravecka, and L. Ribickis, “Model of Laboratory Test Bench Setup for Testing Electrical Machines,” in *2020 IEEE 61th International Scientific Conference on Power and Electrical Engineering of Riga Technical University (RTUCON)*, Riga, Latvia, 2020.

[28] A. Sciarretta and A. Vahidi, Energy-Efficient Driving of Road Vehicles, Cham: Springer International Publishing, 2020, p. 294.

[29] Л. Байрыева and В. Шевченко, Электрическая тяга. Городской наземный, Москва: Транспорт, 1986, p. 206.

[30] В. Розенфельд, И. Исаев, Теория Электрической Тяги, Москва: Транспорт, 1995, p. 294.

[31] I. Dvornikovs, M. Marinbahs, J. Zarembo, E. Groza and K. Ketners, “Investigation of traction motor dynamic using computer simulation and method of mutual loading of two pair motors,” in *2019 16th Conference on Electrical Machines, Drives and Power Systems (ELMA)*, Varna, Bulgaria, 2019.

[32] G. Kobenkins, M. Marinbahs O. Sliskis, V. Burenin, J. Zarembo, “Carry Out of Strength Tests of Geared Motor Box as Part of a Frequency-Controlled Traction

Electric Drive," in *17th Conference on Electrical Machines, Drives and Power Systems (ELMA 2021)*, Sofia, Bulgaria, 2021.

[33] G. Kobenkins, M. Marinbahs, V. Burenin, J. Zarembo, A. Bizans, O. Sliskis, "Determination of the Level of Own Vibration of Geared Motor Boxes in Industrial Conditions," in *2021 IEEE 62st International Scientific Conference on Power and Electrical Engineering of Riga Technical University* , Riga, 2021.

[34] V. Burenin, J. Zarembo, O. Krievs, and L. Ribickis, "Comparison of Synchronous Reluctance Motor and Induction Motor Efficiency Maps for Traction Application," in *RTUCON 2021*, Riga, Latvia, 2021.

[35] H. Kärkkäinen, L. Aarniovuori, M. Niemelä, J. Pyrhönen, and J. Kolehmainen, "Technology comparison of induction motor and synchronous reluctance motor," in *IECON 2017 - 43rd Annual Conference of the IEEE Industrial Electronics Society*, 2017.

[36] A. V. Zakharov, S. I. Malafeev and A. L. Dudulin, "Synchronous reluctance motor: Design and experimental research," in *2018 X International Conference on Electrical Power Drive Systems (ICEPDS)*, 2018.

[37] A. Rassolkin, H. Heidari, A. Kallaste, T. Vaimann, J. P. Acedo, and E. Romero-Cadaval, "Efficiency Map Comparison of Induction and Synchronous Reluctance Motors," in *2019 26th International Workshop on Electric Drives: Improvement in Efficiency of Electric Drives (IWED)*, 2019.

[38] United Nations, "Worldwide Harmonized Light vehicles Test Procedure, Addedndum 15," United Nations, 2019.

Jaroslavs Zarembo was born in 1990 in Liepaja. He received a Bachelor's degree in Electrical Sciences, and a Master's degree in Electrical and Power Engineering from Riga Technical University in 2012, and 2014, respectively. Since 2013, he has been working at JSC "Riga Electric Machine Building Works", where he currently holds a position of Deputy Chief Designer. His research interests are traction drive control and design of inverters and electric motors.